Economic Geology, v. 119, no. 2, pp. 305–329

Tracing Detrital Epidote Derived from Alteration Halos to Porphyry Cu Deposits in Glaciated Terrains: The Search for Covered Mineralization

A. Plouffe,[1,†] R. G. Lee,[2] K. Byrne,[3,*] I. M. Kjarsgaard,[4] D. C. Petts,[1] D.H.C. Wilton,[5] T. Ferbey,[6] and M. Oelze[7,8]

[1]*Geological Survey of Canada, 601 Booth Street, Ottawa, Ontario K1A 0E8, Canada*

[2]*Mineral Deposit Research Unit, The University of British Columbia, 2207-2020 Main Mall, Vancouver, British Columbia V6T 1Z4, Canada*

[3]*Department of Earth and Atmospheric Sciences, University of Alberta, 1-26 Earth Sciences Building, Edmonton, Alberta T6G 2E3, Canada*

[4]*15 Scotia Place, Ottawa, Ontario K1S 0W2, Canada*

[5]*Department of Earth Sciences, Memorial University, 9 Arctic Avenue, St. John's, Newfoundland A1B 3X5, Canada*

[6]*British Columbia Geological Survey Branch, 1810 Blanshard Street, Victoria, British Columbia V8T 4J1, Canada*

[7]*Bundesanstalt Für Materialforschung und-prüfung (BAM), Unter den Eichen 87, Berlin 12205, Germany*

[8]*Helmholtz Centre Potsdam, GFZ German Research Centre for Geosciences, Telegrafenberg, Potsdam 14772, Germany*

Abstract

Distal alteration related to porphyry Cu mineralization is typically characterized by an abundance of green minerals, such as epidote, tremolite, and chlorite, within the propylitic and sodic-calcic alteration zones and extends far outside (>1 km) the mineralized zone(s). Glacial erosion and dispersal derived from rocks affected by propylitic and sodic-calcic alteration have resulted in the development of extensive dispersal trains of epidote in till (glacial sediment) that can reach 8 to 330 km^2 as observed at four porphyry Cu study sites in the Quesnel terrane of south-central British Columbia: Highland Valley Copper, Gibraltar, Mount Polley, and Woodjam deposits. At each of these sites, epidote is more abundant in heavy mineral concentrates of till collected directly over and down-ice from mineralization and associated alteration. Epidote grains in till with >0.6 ppm Sb and >8 ppm As (as determined by laser ablation-inductively coupled plasma-mass spectrometry) are attributed to a porphyry alteration provenance. There is a greater abundance of epidote grains with high concentrations of trace elements (>12 ppm Cu, >2,700 ppm Mn, >7 ppm Zn, and >37 ppm Pb) in each porphyry district compared to background regions. This trace element signature recorded in till epidote grains is heterogeneously distributed in these districts and is interpreted to reflect varying degrees of metal enrichment from a porphyry fluid source. Tracing the source of the epidote in the till (i.e., geochemically tying it to porphyry-related propylitic and/or sodic-calcic alteration), coupled with porphyry vectoring tools in bedrock, will aid in the detection of concealed porphyry Cu mineralization in glaciated terrains.

Introduction

Hydrothermal fluids that lead to the formation of metallic element enrichment are also responsible for the production of alteration halos in the bedrock surrounding porphyry Cu mineralization (Lowell and Guilbert, 1970; Sinclair, 2007; Richards, 2011). The most distal alteration zone surrounding porphyry mineralization, known as propylitic, can be kilometers wide and consist of a variable assemblage including epidote, calcite, albite, chlorite, tremolite, and/or pyrite (Meyer and Hemley, 1967), with sodic-calcic alteration formed on the deep margins of porphyry deposits, including epidote, actinolite, and chlorite (Seedorff et al., 2008). Propylitic and sodic-calcic alteration has recently been referred to as the "green rock environment" by Cooke et al. (2014, 2020a) because of the abundance of green-colored minerals. A special issue of *Economic Geology* (Orovan and Hollings, 2020) presented case studies of porphyry deposits worldwide, emphasizing vectoring toward mineralization and establishing the fertility potential based on the mineral composition (epidote, chlorite) of propylitic and sodic-calcic alteration. This geochemical vectoring technique has potential for mineral exploration, as demonstrated by Cooke et al. (2020b), who reported a case study of the Resolution deposit in Arizona, and by Wilkinson et al. (2020), who presented a study of the El Teniente deposit in Chile. Employing such a mineralogical method can assist in terrains where only the propylitic environment is exposed above or in a distal position from a buried porphyry deposit.

The application of this vectoring method in glaciated terrains with poor bedrock exposure and extensive sediment cover can be challenging, especially during the early stages of mineral exploration when access to bedrock is very limited. We present data sets from four porphyry Cu sites in the Canadian Cordillera (Highland Valley Copper, Gibraltar, Mount Polley, and Woodjam) that demonstrate that the epidote of propylitic and sodic-calcic alteration associated with porphyry Cu mineralization can be identified in till—clastic sediment directly deposited by glaciers—by determining the abundance and composition of detrital epidote. The main challenge in using epidote as an indicator mineral of porphyry mineralization is distinguishing between the two main

[†]Corresponding author: e-mail, alain.plouffe@nrcan-rncan.gc.ca
[*]Present address: Teck Resources Limited, Suite 3300, 550 Burrard Street, Vancouver, British Columbia V6C 0B3, Canada.

ISSN 0361-0128; doi:10.5382/econgeo.5049; 25 p.
Digital appendices are available in the online Supplements section.

Submitted: December 21, 2022 / Accepted: May 24, 2023

sources of epidote in the study area: epidote derived from the alteration zones associated with porphyry Cu mineralization and epidote derived from regionally metamorphosed rocks of the Nicola Group. The distinction between these two broad types is further complicated by the fact that some of the epidote-bearing metamorphic rocks near the intrusion might have been overprinted by hydrothermal fluids associated with porphyry mineralization. Furthermore, epidote associated with the alteration assemblage of a mineralized porphyry Cu system needs to be discriminated from epidote from barren hydrothermal systems. This paper presents an overview of how the abundance of epidote in till and its composition can be used to detect the potential presence of buried porphyry mineralization. Geochemical indicators from epidote composition that may have utility in exploration are also discussed.

Geologic Setting

The Cordillera of British Columbia has long been known for its wealth of porphyry mineralization (Sutherland Brown, 1976; Schroeter, 1995; Logan and Schroeter, 2013; Sharman et al., 2020). Across Canada, 40% of Cu production comes from porphyry deposits (Sinclair, 2007). Copper accounts for 28% of the total value of all mineral production in British Columbia, the majority of which is produced from porphyry Cu deposits (Clarke et al., 2021), largely located in the Quesnel and Stikine terranes with a limited number within the Wrangell terrane (Fig. 1). These terranes are composed of rocks of island-arc affinities, which were accreted to North America during the Mesozoic. Most of the porphyry mineralization formed in intrusive rocks during two broad time windows: a preaccretionary period, which was the most prolific, from Late Triassic to Early to Middle Jurassic, and a postaccretionary period, from Cretaceous to Eocene. The period from 208 to 204 Ma was particularly productive, accounting for 90% of the known porphyry deposits in British Columbia (Logan and Mihalynuk, 2014). In an assessment of porphyry Cu mineralization in the Canadian Cordillera based on 2010 data, Mihalasky et al. (2011) estimated that approximately 49 million tonnes (Mt) of Cu in porphyry deposits remains undiscovered.

The research presented here assembles data sets from four porphyry study sites in British Columbia: the Highland Valley Copper porphyry Cu-Mo, the Gibraltar porphyry Cu-Mo, the Mount Polley porphyry Cu-Au ± Ag, and the Woodjam porphyry Cu-Au ± Mo deposits (Fig. 1). Mining by open pit has occurred at all sites except Woodjam. All are hosted in Late Triassic to Early Jurassic mafic to felsic intrusive rocks that intruded the Upper Triassic Nicola Group succession of island-arc volcanic and sedimentary rocks, the main constituent of the Quesnel terrane. The intrusive bodies that host mineralization include the Guichon Creek batholith at Highland Valley Copper, the Granite Mountain batholith at Gibraltar, the Mount Polley Intrusive Complex at Mount Polley, and the Takomkane batholith and associated satellite intrusions at Woodjam (Fig. 2). The deposits vary substantially in size

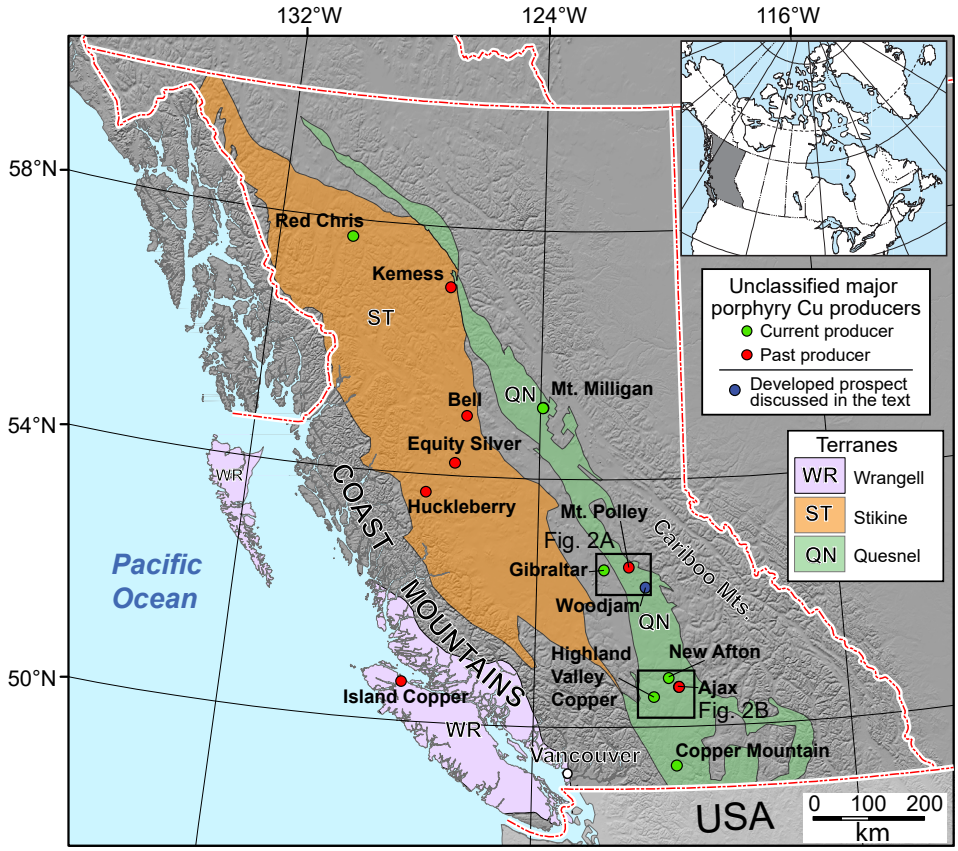

Fig. 1. Inset with location of British Columbia in Canada (gray area). Quesnel, Stikine, and Wrangellia terranes in British Columbia with the unclassified major past and current porphyry Cu producers. The figure shows the location of the four study sites: Highland Valley Copper, Gibraltar, and Mount Polley deposits and the Woodjam prospect.

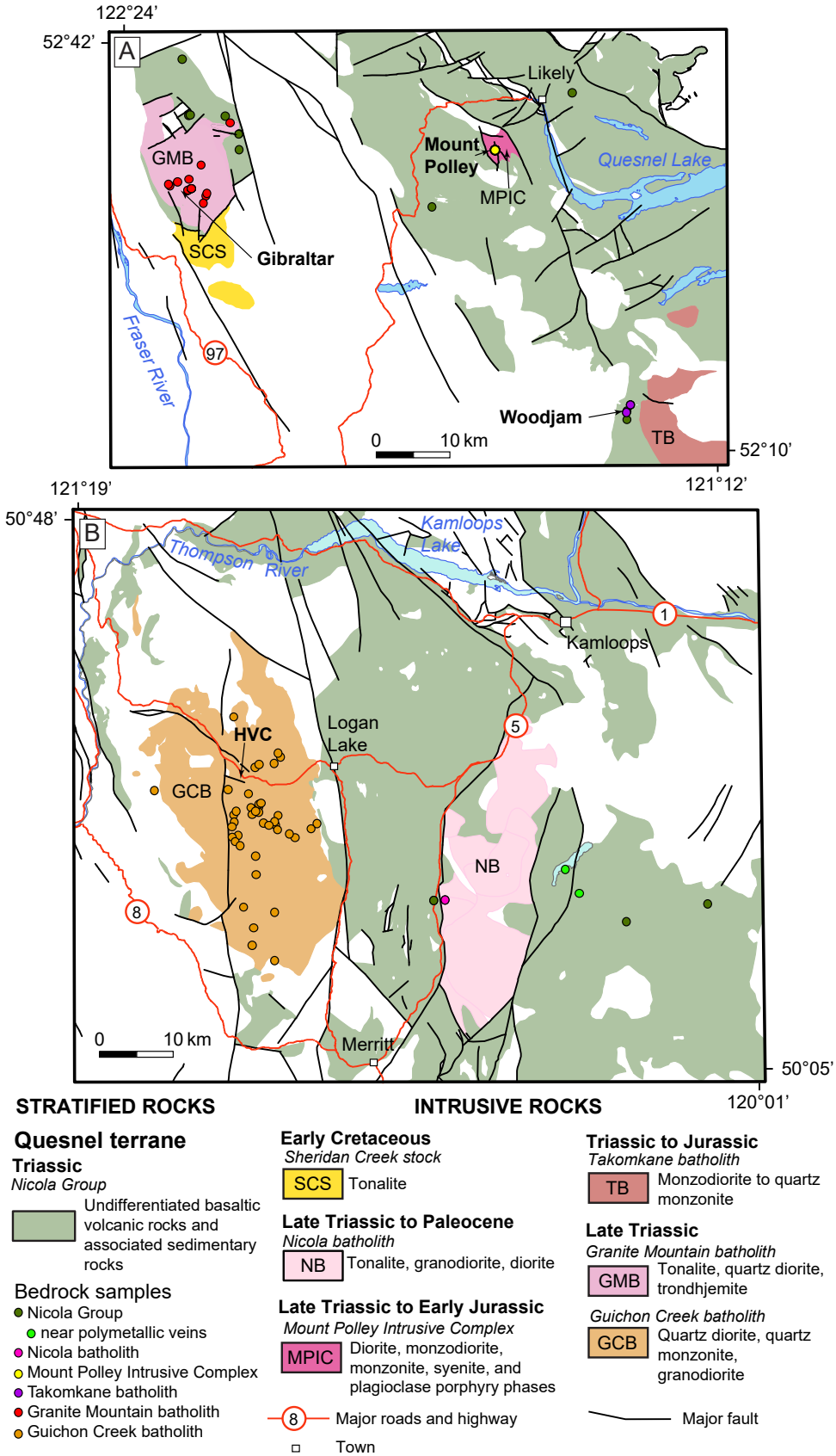

Fig. 2. Regional geology from Cui et al. (2017) for (A) Gibraltar, Mount Polley, and Woodjam and (B) Highland Valley Copper (HVC) deposits. The locations of the bedrock samples that were analyzed as part of this study are shown.

(mined and resources) but have a similar tenor of mineralization: at Highland Valley Copper there is a total of 338.3 Mt of proven and probable reserves at 0.31% Cu and 0.008% Mo (Teck, 2022); 1.44 billion tonnes of ore at 0.3% Cu and 0.009% Mo at Gibraltar (van Straaten et al., 2020); 172 Mt of ore at 0.2 to 0.3% Cu (but up to 1.14% Cu in the Martel underground zone) and 0.2 to 0.3 g/t Au at Mount Polley (Rees et al., 2020); and 275 Mt of ore at 0.1 to 0.3% Cu and 0.3 to 0.7 g/t Au distributed within four mineralized zones at Woodjam (Sherlock and Trueman, 2013; Sherlock et al., 2013; del Real et al., 2017, 2020). Only at the Gibraltar deposit are the mineralized rocks deformed in ductile shear zones (van Straaten et al., 2020). Postmineralization regional metamorphism reached prehnite-pumpellyite facies at Highland Valley Copper, zeolite facies at Mount Polley and Woodjam, and greenschist facies at Gibraltar (Greenwood et al., 1991; Panteleyev et al., 1996).

The regional alteration in bedrock has been mapped relative to mineralization at Highland Valley Copper (Byrne, 2019; Byrne et al., 2020b) and Mount Polley (Rees et al., 2020) (Fig. 3A, B, E, F). At Highland Valley Copper there are two dominant sources of bedrock epidote recognized: epidote veins with K-feldspar destructive albite and chlorite ± actinolite halos that are interpreted as sodic-calcic alteration, and prehnite ± epidote veins with K-feldspar-stable illite-chlorite-prehnite ± epidote halos that are interpreted as propylitic alteration (Byrne et al., 2020a). The most intense sodic-calcic alteration (mapped vein and halo density of >1.25 cm/m) and propylitic alteration (mapped vein and halo density of >0.5 cm/m) are centered on the porphyry Cu-Mo mineralization and together have a footprint of approximately 34 km² (Fig. 3A; Byrne, 2019). The veins are steeply dipping (>70°) and generally strike parallel to the alteration zones (Byrne et al., 2020b). Although these represent the dominant source of epidote, other possible sources include wall rock that has undergone widespread propylitic alteration associated with emplacement of multiple, premineralization phases of Guichon Creek batholith that occur beyond the most intensely altered zones (Fig. 3A, B; Byrne et al., 2020b). Alteration zone IV of Rees et al. (2020) (Fig. 3E, F), along the southern margin of the Mount Polley Intrusive Complex, comprises albite, epidote, chlorite, and pyrite and is the principal source of epidote, although epidote also occurs in lesser amounts in the other alteration zones throughout the Mount Polley Intrusive Complex (zones I, II, and III of Rees et al., 2020).

Not all intrusions in the Quesnel terrane were fertile (i.e., produced porphyry deposits). Our assessment of epidote composition as an indicator of porphyry Cu mineralization

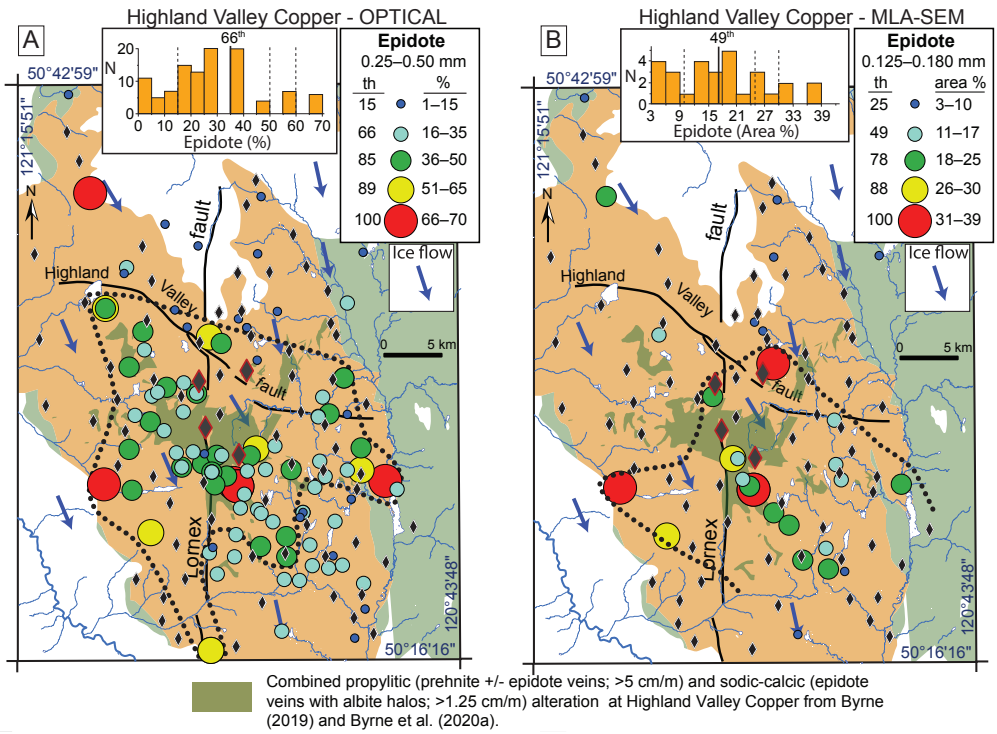

Fig. 3. Epidote abundance in till from the four porphyry Cu sites determined by optical and mineral liberation analysis-scanning electron microscope (MLA-SEM) methods: (A, B) Highland Valley Copper; (C, D) Gibraltar; (E, F) Mount Polley; and (G, H) Woodjam. The optical method provides the percentage of epidote grains in heavy mineral concentrates (0.25–0.50 mm; >3.2 specific gravity [SG]) and the MLA-SEM method the area percent of epidote over the total mineralogical surface of a 30-mm-diameter circular grain mount (0.125–0.180 mm; >3.2 SG). Results on epidote abundance in till were first published in Plouffe et al. (2021b). More samples were analyzed since then, and all results are provided in Appendix Table A1. The simplified bedrock geology is derived from McMillan et al. (2009) at Highland Valley Copper, Massey et al. (2005) and Schiarizza (2015) at Gibraltar, Massey et al. (2005) and Rees et al. (2020) at Mount Polley, and Massey et al. (2005) and Logan et al. (2010) at Woodjam. Each map includes a histogram with a vertical black line that defines the threshold between background and anomalous abundances of epidote. The dashed lines in the histograms correspond to the percentile class breaks (th) used in the legend. The dotted line on the maps outlines the areal extent of the glacial dispersal of epidote based on the distribution of samples with anomalous abundances. The bedrock geology legend is the same as shown in Figure 2.

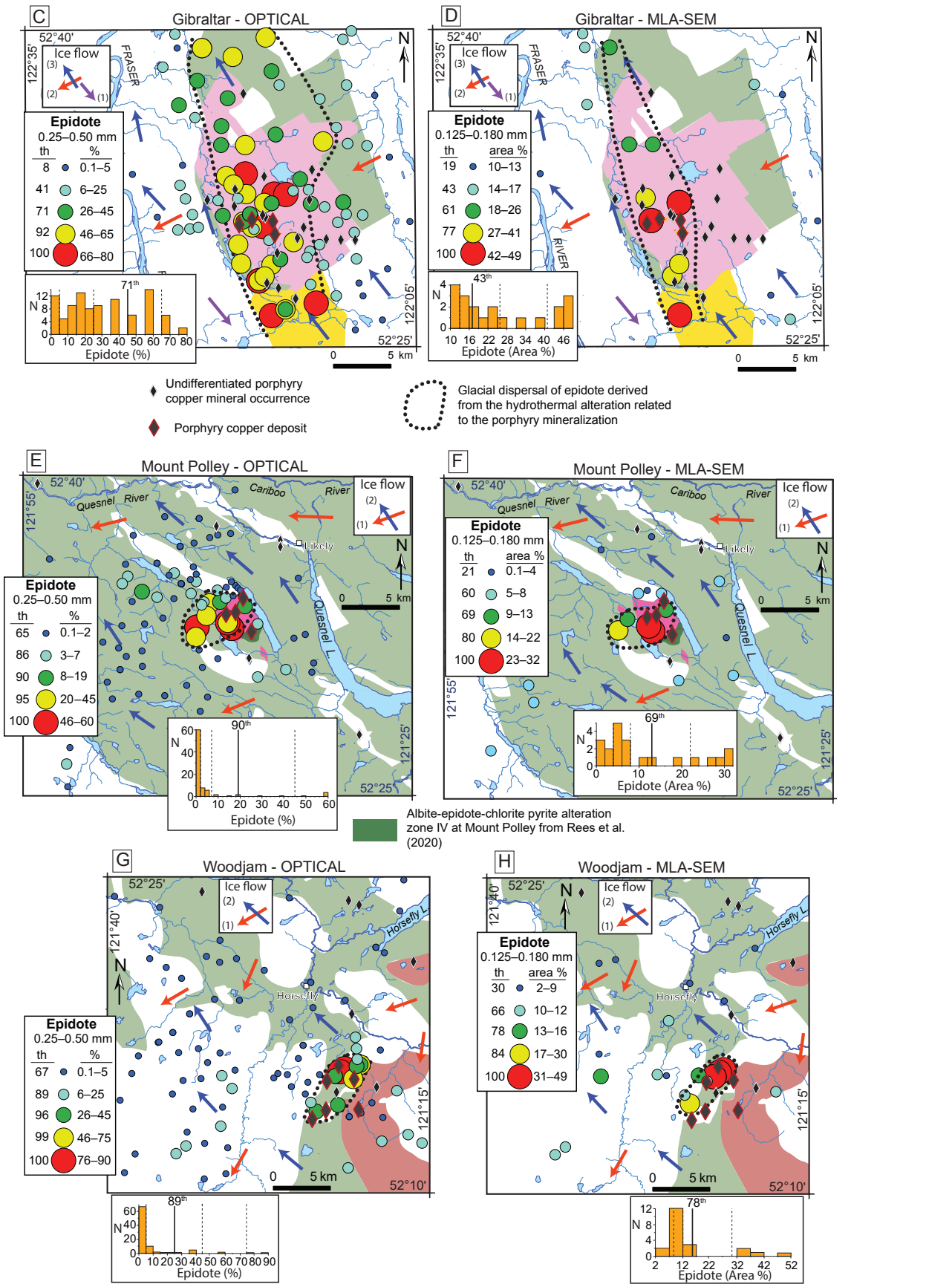

Fig. 3. *(Cont.)*

includes samples from the Nicola batholith (Fig. 2), which contain weak replacement of plagioclase by epidote and a low abundance of epidote-bearing veins (D'Angelo, 2016; Byrne, 2019). The Nicola batholith consists of a suite of mafic and felsic Late Triassic to Paleocene intrusive rocks (230–64 Ma) exposed in a horst approximately 20 km east of the Guichon Creek batholith (Erdmer et al., 2002). Except for the Paleocene intrusive rocks in the batholith, all rock types have undergone upper greenschist to lower amphibolite metamorphism (Erdmer et al., 2002; D'Angelo, 2016). Based on criteria established by Loucks (2014) using whole-rock geochemistry, D'Angelo (2016) considers the Nicola batholith to be potentially fertile for porphyry mineralization. However, porphyry mineral showings in the Nicola batholith are limited and are located only in the southern part of the intrusion (British Columbia Geological Survey, 2020). The southern sector of the intrusion contains one past-producing porphyry Cu deposit, the Turlight mine, which yielded approximately 180 t of ore grading 5 to 6% Cu from 1948 to 1956 (Minfile 092ISE055: British Columbia Geological Survey, 2020). Our compilation includes samples of epidote veins from the Nicola batholith obtained approximately 25 km north of the Turlight mine, where there is no known porphyry mineralization (Byrne, 2019); these samples are considered to represent a barren intrusive hydrothermal system. However, we cannot completely disregard the possibility that porphyry mineralization could be present at depth in the intrusion, proximal to the sampling sites.

Our compilation also includes epidote-bearing samples from the Nicola Group volcanic and sedimentary rocks that have been metamorphosed to greenschist facies following regional burial metamorphism (Greenwood et al., 1991). These samples establish the composition of background epidote for comparison to porphyry-related epidote. Also included are two samples of epidote veins collected <1.5 km from polymetallic (Ag-Pb-Zn ± Au) vein occurrences approximately 30 km east of the Guichon Creek batholith.

Glacial History

A brief overview of the glacial history and ice-flow movements in the study area is necessary to interpret the glacial dispersal patterns observed in the till. All study sites were glaciated from about 25 to 10.5 k.y. Before Present during the Late Wisconsin glaciation (Dyke, 2004; Clague and Ward, 2011). The first of the four study sites to be glaciated was likely the Gibraltar deposit, with ice flowing toward the south to southeast from a mountainous ridge located 13 km north of the mine site, as marked by cirques and arêtes (Plouffe et al., 2022). This first southerly ice movement was followed by ice moving toward the west to southwest, from the Cariboo Mountains to the east (Fig. 1). The third and last regional ice movement occurred toward the north to northwest when ice from the Coast and Cariboo mountains coalesced over the Interior Plateau during the glacial maximum, creating an ice divide at about latitude 52° N (Arnold et al., 2016; Arnold and Ferbey, 2020). Only the second and third ice movements (west to southwest followed by north to northwest) affected the Woodjam and Mount Polley regions. The ice-flow history at Highland Valley Copper is relatively simpler, with only a single ice movement toward the south to southeast derived from the ice divide at latitude 52° N (Arnold et al., 2016; Plouffe and Ferbey, 2018; Arnold and Ferbey, 2020).

Porphyry Cu Indicator Minerals in Till

Plouffe and Ferbey (2017) provide an overview of the key porphyry Cu indicator minerals that can be identified in till and other detrital sediments. These minerals in till can be directly linked to the potential presence of porphyry Cu mineralization in bedrock of the provenance region, which is in the region up-ice of the movements of glaciers. These indicator minerals can be separated from the till matrix by sieving and by density and magnetic separations. These mineral grains must be robust enough to survive glacial processes (e.g., abrasion, comminution) and postglacial weathering following till deposition (Plouffe and Ferbey, 2017).

Plouffe and Ferbey (2017) classify porphyry Cu indicator minerals into two broad categories. Group 1 minerals are more abundant in till near porphyry mineralization, or its associated alteration zones, and decrease in abundance with increasing distance of glacial transport. By itself, the abundance of these minerals in till directly suggests the presence of porphyry Cu mineralization up-ice. Examples of group 1 minerals include chalcopyrite, which is the dominant Cu sulfide in porphyry Cu mineralization (e.g., Kelley et al., 2011; Plouffe et al., 2016), and gold grains from porphyry Cu-Au mineralization (Hashmi et al., 2015). In contrast, the abundance and distribution of group 2 minerals in till are not directly linked to the presence of mineralization; such links are better established using mineral chemistry. Examples of group 2 minerals that can have chemical signatures indicative of porphyry mineralization include magnetite (Pisiak et al., 2017), apatite (Rukhlov et al., 2016; Mao et al., 2017), tourmaline (Beckett-Brown et al., 2023a, b), and zircon (Lee et al., 2021). The details of this two-group classification scheme for porphyry Cu indicator minerals are site-specific and dependent on the mineralogy of the porphyry system exposed to glacial erosion.

At the four porphyry study sites described here, epidote classifies as group 1 because, as demonstrated below, it is more abundant in till down-ice of propylitic alteration zones associated with porphyry mineralization. However, there are other regional bedrock sources of epidote near these study sites that are unrelated to porphyry systems. Mineral chemistry is used to differentiate epidote from porphyry systems from that sourced from regional bedrock.

Epidote: Background and Previous Studies

The epidote supergroup is part of the sorosilicates with the general formula $A_2M_3[T_2O_7][TO_4](O,F)(OH,O)$ (Armbruster et al., 2006). A wide range of elements can substitute in epidote (Frei et al., 2004), including di- and trivalent cations in the A site (e.g., Ca^{2+}, Mn^{2+}, Sr^{2+}, Pb^{2+}, rare-earth elements $[REE]^{3+}$) and trivalent cations in the M site (e.g., Al^{3+}, Fe^{3+}, REE^{3+}) (Armbruster et al., 2006). Armbruster et al. (2006) and Mills et al. (2009) subdivide the epidote supergroup into three groups: epidote, allanite (REE-rich), and dollaseite (Mg equivalent of allanite). Epidote $[Ca_2Al_2Fe^{3+}[Si_2O_7][SiO_4]O(OH)]$ and clinozoisite $[Ca_2Al_3[Si_2O_7][SiO_4]O(OH)]$, the Fe- and Al-rich end members, form a solid solution.

Epidote is a common rock-forming mineral in alteration zones associated with porphyry systems (Meyer and Hemley,

1967; Cooke et al., 2014). It can occur as a replacement product (e.g., after plagioclase or hornblende) or as a direct precipitate of hydrothermal fluids, typically present in fractures and veins (Lowell and Guilbert, 1970; Sillitoe, 2010). It can also occur in nonmineralized hydrothermal systems (Bird et al., 1984; Bird and Spieler, 2004) and in metamorphic rocks from upper zeolite to intermediate amphibolite facies but is most common in greenschist facies rocks (Grapes and Hoskin, 2004). Epidote can be present in unconsolidated detrital sediments, including glacial deposits (e.g., Hashmi et al., 2015; Plouffe et al., 2016; Plouffe and Ferbey, 2017), indicating that it has survived glacial comminution and postglacial weathering, in part because of its hardness of 6 to 7 and stability in surficial weathering environments (Berry et al., 1983).

Previous studies reported variable concentrations of trace elements (e.g., Mn, Cu, Zn, As, Sn, Sb, Pb) in epidote from porphyry systems (e.g., Bowman et al., 1987; Norman et al., 1991; Cooke et al., 2014). These elements occur in elevated and spatially variable concentrations that correlate with the distance from the porphyry centers—gradients that can be used to vector toward porphyry Cu mineralization (Cooke et al., 2014, 2020a, b; Jago et al., 2014; Byrne, 2019; Baker et al., 2020; Wilkinson et al., 2020). A simple bivariate plot of As versus Sb provides some indication of the origin of the epidote because hydrothermal epidote that formed in porphyry alteration zones contains higher concentrations of these pathfinder elements compared to metamorphic epidote (Wilkinson et al., 2017, 2020; Byrne, 2019; Baker et al., 2020; Cooke et al., 2020b). The reported enrichment of Cu and Sn in epidote gradually decreases with increasing distance from porphyry ore (proximal pathfinder elements), as opposed to the enrichment of Mn, Zn, As, Sb, and Pb, which show the opposite trend of increase in concentrations with increasing distance (distal pathfinder elements). The regional distribution of chalcophile elements in porphyry-related epidote is controlled by the presence of pyrite in the alteration halo of the porphyry deposit (Cooke et al., 2014). The presence of pyrite reduces the concentrations of these elements in epidote, since they preferentially partition into pyrite. These trace element anomalies are observed in vein and replacement epidote (Cooke et al., 2014), with distinct differences between both epidote types in site-specific studies (Byrne, 2019; Ahmed et al., 2020). The strength of the pathfinder element anomalies is correlated with the flux of metals in the parental hydrothermal fluids, which is argued to indicate the fertility of the porphyry mineralizing event (Cooke et al., 2014).

Epidote: Forms and Distribution at the Four Study Sites

An extensive description of the style of epidote alteration and its chemical composition at the Guichon Creek batholith at Highland Valley Copper was provided by Byrne (2019) and Byrne et al. (2020a, b). In the Highland Valley district, epidote predominantly occurs in the sodic-calcic and propylitic alteration zones, as described above. Minor sulfides were observed only in epidote veins in the propylitic alteration zone.

Kobylinski et al. (2017) discuss the styles of epidote alteration in the Granite Mountain batholith, the Sheridan Creek stock, and the Nicola Group volcanic rocks of the Gibraltar deposit region. Disseminated epidote is present in all intrusive phases of the Granite Mountain batholith, whereas epidote veins are present in the batholith, the Sheridan Creek stock, and the nearby Nicola Group rocks. Some of the veins in the Granite Mountain batholith and the Nicola Group rocks display features related to the ductile deformation of these rocks (Schiarizza, 2015; Kobylinski et al., 2017). The veins and veinlets are <1 mm to 15 cm wide and are composed of epidote, quartz, and chlorite. Kobylinski et al. (2017) noted epidote veins as far as 10 km from mineralization. Disseminated epidote, partly or completely replacing plagioclase, occurs in all phases of the Granite Mountain batholith up to 5 km from the main mineralized zones.

At Mount Polley, epidote occurs as fine-grained disseminations and veinlets with calcite in alteration zones extending throughout the Mount Polley Intrusive Complex. Epidote is most abundant at the southern limit of the intrusive complex and within the Nicola Group rocks, near the intrusive contact (Fraser et al., 1993, 1995; zone IV of Rees et al., 2020).

At Woodjam, vein and disseminated epidote is present in the five deposits. Various alteration zones containing epidote (e.g., albite-epidote, chlorite-epidote) typically overprint K-silicate alteration and predominate on the periphery of mineralization within the intrusive rocks, which extend outward into the Nicola Group (del Real et al., 2017, 2020).

Methods

Intrusive bedrock samples containing epidote were collected from outcrops at the four porphyry study sites and from the Nicola batholith (Fig. 2). Nicola Group rock samples were collected distal (approximately >5 km) and proximal (approximately <1 km) to the porphyry centers and polymetallic vein mineralization (Fig. 2). Polished sections were prepared from the rock samples for laser ablation-inductively coupled plasma-mass spectrometry (LA-ICP-MS) analysis.

Field methods for collecting till samples and laboratory methods for the recovery of heavy mineral concentrates are described in Plouffe and Ferbey (2016) and Ferbey et al. (2016). The abundance of epidote in the till was determined using two methods. First, epidote was identified under a binocular microscope at Overburden Drilling Management Ltd. (Ottawa, Canada). The results are reported as a percentage of epidote in the heavy mineral concentrates of the 0.25- to 0.50-mm size with >3.2 specific gravity (SG) fraction. This optical method has a precision of ±10% based on replicate analyses (Plouffe and Ferbey, 2016). Partial results of the epidote abundance determined by this optical method were presented in Plouffe et al. (2021b). The complete results are depicted on maps in this paper and provided in the Appendices (Table A1). Second, epidote abundance was also determined in the 0.125- to 0.180-mm size with >3.2-SG fraction using a scanning electron microscope (SEM) linked to a mineral liberation analysis (MLA) database. These analyses were completed at the Core Research Equipment and Instrument Training (CREAIT) microanalysis facility at Memorial University (St. John's, Canada). In this case, the results are reported as the area percent of epidote over the total mineralogical surface of a 30-mm-diameter circular grain mount (App. Table A1). Empty spaces between mineral grains are not considered. The details of the MLA-SEM methodology are presented in Plouffe et al. (2021b). The analytical

precision of MLA-SEM analyses, based on replicate analytical runs of the same sample using proper calibration measures, is <±1% (Lougheed et al., 2020). The number of samples processed by both methods is provided in Table 1. Fewer samples were processed by MLA-SEM than by the optical method. Therefore, detailed interpretation of glacial dispersal by the MLA-SEM methodology is limited. However, a general identification of the regional abundance of epidote in till near porphyry mineralization is possible.

The geochemical analysis of till samples to detect the footprint of ore and pathfinder elements down-ice of porphyry deposits, which is an intrinsic part of this study, has been presented elsewhere (Hashmi et al., 2015; Plouffe et al., 2016, 2022; Shewchuk et al., 2020).

LA-ICP-MS was used to determine the composition of epidote from three sample types: (1) hydrothermally altered intrusive bedrock samples from the four porphyry deposits (Highland Valley Copper, n = 41; Gibraltar, n = 10; Mount Polley, n = 10; Woodjam, n = 7) and the barren Nicola batholith (n = 2), (2) metamorphosed volcanic and volcaniclastic bedrock samples from the Nicola Group (n = 16), including two samples collected near polymetallic vein mineralization, and (3) detrital grains recovered from subglacial till samples collected from various locations up-ice and down-ice of porphyry mineralization at the four study sites (Table 1). Disseminated and vein epidote compositions were determined for all bedrock samples, except those from Highland Valley Copper. Given the limited number of LA-ICP-MS analyses for replacement epidote from Highland Valley Copper (Byrne, 2019), only vein epidote is considered in this study, which represents the greater proportion of epidote in the intrusion.

These LA-ICP-MS analyses were completed in three laboratories: the Geological Survey of Canada (GSC; Ottawa, Canada), the Pacific Centre for Isotopic and Geochemical Research at the University of British Columbia (PCIGR-UBC; Vancouver, Canada), and the German Research Centre for Geosciences (GRCG; Postdam, Germany) (Table 2). Analytical results and procedures are presented in the Appendices (Table A2 and App. 1, respectively).

Mapping of epidote in polished sections and mounted grains from till samples was completed at the GSC using LA-ICP-MS. A detailed description of the mapping procedure, which follows the previously published protocols of Lawley et al. (2015, 2020) and Paradis et al. (2020), is provided in Appendix 1.

Table 1. Number of Till Samples Processed for Epidote Abundance by Optical and MLA-SEM Methods and for Epidote Composition by LA-ICP-MS

Study site	Optical method (0.25–0.50 mm; >3.2 SG)	MLA-SEM (0.125–0.180 mm; >3.2 SG)	LA-ICP-MS (0.25–0.50 mm; >3.2 SG)
Highland Valley Copper	108	29	10
Gibraltar	95	20	10
Mount Polley	86	20	9
Woodjam	91	21	7

Abbreviations: LA-ICP-MS = laser ablation-inductively coupled plasma-mass spectrometry, MLA-SEM = mineral liberation analysis-scanning electron microscope, SG = specific gravity

Table 2. List of Laboratories and Type of Samples Analyzed at Each Laboratory

LA-ICP-MS laboratory	Samples
GSC (Ottawa, Canada)	Epidote in intrusive rock samples from Gibraltar, Mount Polley, and Woodjam and from Nicola Group rocks; till epidote from Gibraltar, Mount Polley, and Woodjam
PCIGR-UBC (Vancouver, Canada)	Till epidote from Highland Valley Copper
GRCG (Potsdam, Germany)	Epidote in intrusive rocks from Highland Valley Copper and the Nicola batholith, epidote from two Nicola Group rocks near Highland Valley Copper

GRCG = German Research Centre for Geosciences, GSC = Geological Survey of Canada, LA-ICP-MS = laser ablation-inductively coupled plasma-mass spectrometry, PCIGR-UBC = Pacific Centre for Isotopic and Geochemical Research at the University of British Columbia

Results

Results from this study are divided into three broad categories: epidote abundance in till, petrographic comparison of the epidote, and geochemical compositions as revealed by LA-ICP-MS analysis.

Epidote abundance in till

The abundance of epidote in till samples from the four study sites, determined by the optical and MLA-SEM methods, is shown in Figure 3. Broad epidote anomalies in till are generally centered on mineralization and extend from 8 km² at Woodjam and Mount Polley to approximately 330 km² at Highland Valley Copper (Fig. 3). These mineralogical anomalies extend in the direction of the ice flow. For example, the epidote anomaly in till at Highland Valley Copper extends at least 10 km down-ice (to the south southeast) from the zone of alteration and about 4 km down-ice (southwest and northwest) at Mount Polley. At Gibraltar (Fig. 3C, D; Plouffe et al., 2022), the epidote anomaly extends at least 16 km to the north of the deposits, corresponding to the direction of ice movement at glacial maximum (Plouffe et al., 2022). There, the presence of elevated epidote abundances in till to the south, over the Sheridan Creek stock, could be related to the epidote in the underlying intrusion (Ash and Riveros, 2001). These mineralogical anomalies can be identified in the >3.2-SG fraction of the 0.25- to 0.50-mm (optical method) and the 0.125- to 0.180-mm (MLA-SEM) size fractions of till. However, more samples were analyzed by the optical method, providing a better-defined regional coverage.

Based on the distribution patterns of epidote in till at the four study sites, we interpret the main sources to be the hydrothermal alteration zones associated with the porphyry deposits. Variability in epidote abundance in till relates to the epidote distribution in bedrock. For example, the greater abundance of epidote in till at the eastern margin of the Guichon Creek batholith (>51%; Fig. 3A) at Highland Valley Copper corresponds to propylitic alteration in the marginal mafic phase of the intrusion (Byrne et al., 2020a, b). Some of the epidote in the till is also derived from the Nicola Group rocks, as shown

by its abundance of 0.1 to 25% in regions underlain by these rocks up-ice and distal to the porphyry deposits (>10 km). To differentiate the detrital epidote derived from porphyry hydrothermal alteration from that derived from regionally metamorphosed rocks of the Nicola Group, petrographic and geochemical methods were applied.

Petrographic description of epidote

Petrographic examination of the epidote provides some indication of its origin. The massive and coarse euhedral to anhedral epidote in veins within intrusive rocks that host porphyry mineralization (Fig. 4A, B) is interpreted as being hydrothermal in origin. In plane-polarized light, this epidote is olive green and yellow green to brown and has a pitted texture with abundant mineral inclusions, quartz, carbonate, actinolite, titanite, and sulfides being the most common. Some of the epidote in the veins forms prismatic crystals as long as 2 mm. Sulfide inclusions are observed in the epidote within the veins and, in the case of Mount Polley, magnetite can also be present (Fig. 4C). These inclusions were avoided during the LA-ICP-MS analyses. Backscattered electron (BSE) images show compositional zoning within vein epidote that reflects varying degrees of Fe-Al substitution (Fig. 5A). In the Granite Mountain batholith, the epidote veins themselves are zoned, with Fe-poor borders [10.57 wt % Fe_2O_3(total)] and Fe-rich cores [16.52 wt % Fe_2O_3(t)] (Kobylinski et al., 2017).

Epidote also forms crystal aggregates with diameters that reach decimeters and constitutes up to 80% volume of the intrusive rock and therefore, qualifies as epidosite. In these aggregates, epidote occurs as individual anhedral to euhedral crystals with diameters as large as 0.5 mm and is typically intergrown with quartz, carbonate, amphibole, titanite, or minor sulfides (Fig. 4D). Likewise, these aggregates are interpreted to have formed from hydrothermal fluids.

Epidote texture in rock samples of the Granite Mountain batholith is complex and may be related to a combination of porphyry hydrothermal alteration and postmineralization metamorphism. Epidote (>0.1 mm) and titanite replacing chlorite following biotite alteration is interpreted to be related to the porphyry hydrothermal alteration (Fig. 4E). On the other hand, fine-grained (typically ≤0.1 mm) poikilitic epidote overprinting plagioclase (Fig. 4F) was observed in a number of the rock samples from the Granite Mountain batholith and may be of metamorphic origin. Poikilitic epidote overprinting plagioclase is also observed in the Mount Polley Intrusive Complex (Fig. 4G). However, its close association with titanite, magnetite, and pyrite, all part of the hydrothermal alteration mineral assemblage (Rees et al., 2020), suggests that it is of hydrothermal origin.

Poikilitic epidote that overprints plagioclase, chlorite, or carbonate in the Nicola Group rocks forms crystals that are generally <0.05 mm in diameter but can be up to 0.25 mm and can form aggregates as large as 1 mm in diameter (Fig. 4H). This poikilitic epidote occurs as a pale yellow greenish to dark fuzzy mineral grains in plane-polarized light, but some of the crystals appear anhedral to euhedral in reflected light (Fig. 4I). In BSE images, this poikilitic epidote does not show prominent Fe-Al zoning (Fig. 5B), as was observed in epidote from the intrusive rocks, suggesting that it formed in more stable conditions. Based on these observations, this form of epidote found in the Nicola Group rocks is interpreted to be of metamorphic origin. In addition, epidote veins and veinlets that cut the intrusive rocks associated with the porphyry deposits do extend in places into the adjacent Nicola Group rocks. Epidote in these veins and veinlets is yellow green to yellow orange, is dominantly anhedral, and shows Fe-Al zonation in BSE images (Fig. 5C). These epidote veins within the Nicola Group rocks are interpreted to have resulted from hydrothermal alteration associated with the porphyry mineralization.

The majority of the epidote grains recovered from the till samples have characteristics similar to those of the hydrothermal epidote described above. These epidote grains contain inclusions of quartz, carbonate, actinolite, titanite, and sulfides and show Fe-Al zoning in BSE images (Fig. 5D-F). Fractures are observed in some grains (Fig. 5F), potentially resulting from crushing during glacial erosion and transport.

Epidote geochemical composition

There are broad compositional fields for differentiating epidote derived from metamorphism versus porphyry-related hydrothermal activity (Fig. 6; Wilkinson et al., 2017, 2020; Baker et al., 2020; Cooke et al., 2020b). Epidote from the porphyry field contains >0.6 ppm Sb and >8 ppm As. At Highland Valley Copper, 56% of epidote samples from the Guichon Creek batholith falls exclusively in the porphyry-alteration field, excluding epidote with high As and Sb, which falls outside the metamorphic and porphyry-alteration fields. The percentage that falls within the porphyry-alteration field is higher at Mount Polley (96%) and Woodjam (93%) than at Gibraltar (10%), which is characterized by epidote containing generally lower As concentrations than at these other three sites (Fig. 6). There is a general positive correlation between As and Sb concentrations in the epidote from all the sites except for Highland Valley Copper, where this correlation is less apparent (Fig. 6A). High As and Sb concentrations are noted in vein or replacement epidote at the four study sites except at Gibraltar, where As concentrations are low (Fig. 7A, B). Lower As and Sb concentrations are observed in epidote from Nicola Group rocks, including samples collected near (<1.5 km) polymetallic vein mineralization (Figs. 6E, 7A, B). Some of the epidote from samples of Nicola Group bedrock, which were collected <2 km from the porphyry intrusions at Gibraltar and Woodjam (Fig. 2), also contain elevated As and Sb concentrations that are most likely related to the porphyry hydrothermal alteration (Figs. 6E, 7A, B). In the barren Nicola batholith, epidote has low As and Sb concentrations, with 12 of the 16 analyses falling in the metamorphic field or within the overlap between the metamorphic and porphyry-alteration fields (Fig. 6E).

Seventy-one percent of the As and Sb concentrations for epidote grains from the till at Highland Valley Copper, 54% from Gibraltar, 78% from Mount Polley, and 70% from Woodjam fall exclusively within the porphyry-alteration field (Fig. 6A-D). At Gibraltar, abundant epidote grains from till contain higher As concentrations than those observed in the epidote from the intrusive rocks, suggesting that the bedrock samples used in this study do not reflect the full range of the composition of porphyry-related epidote in the Granite Mountain batholith (Fig. 6B). The regional distribution of epidote grains

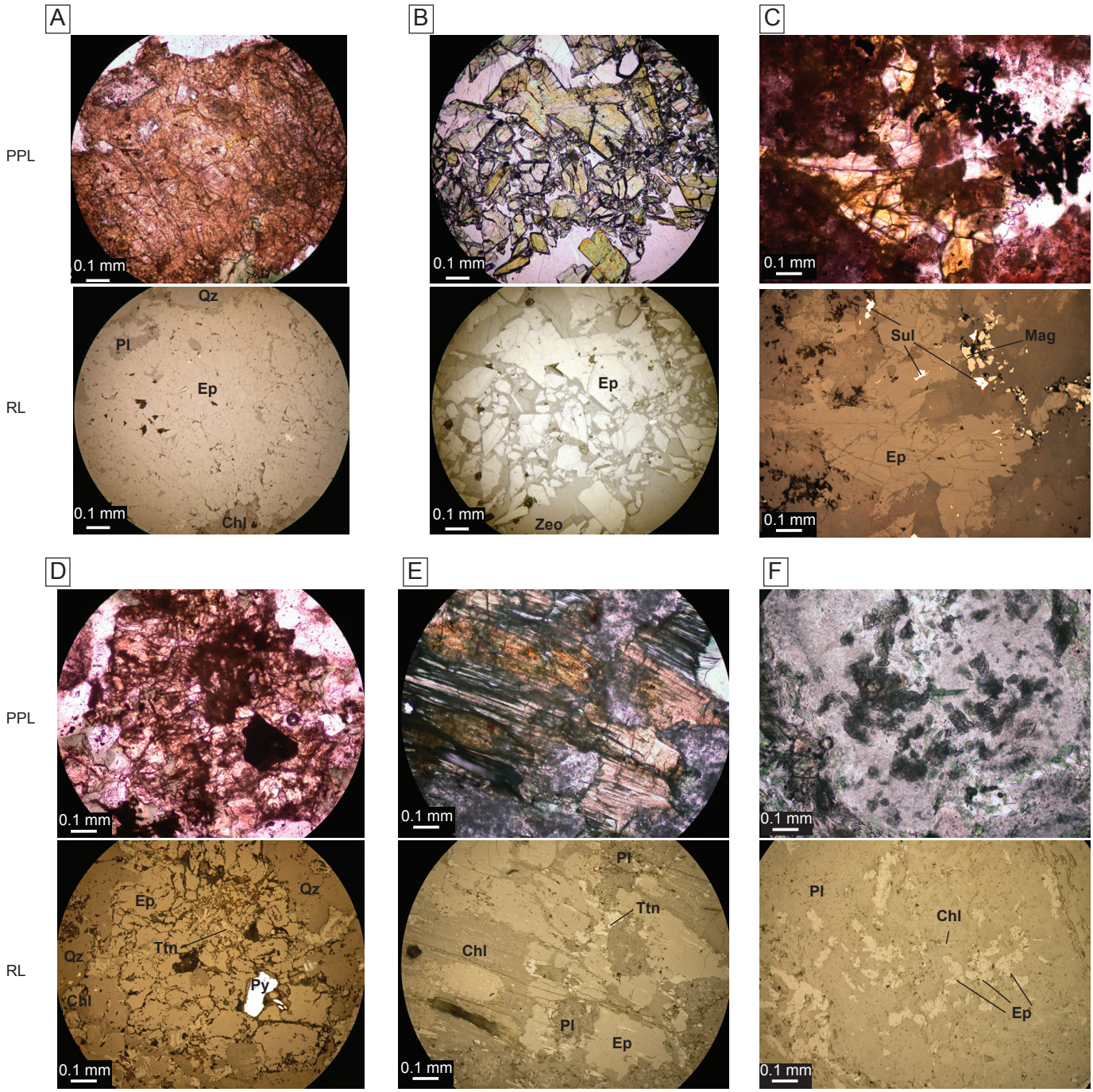

Fig. 4. Paired petrographic photographs in plane-polarized light (PPL) and reflected light (RL) of epidote in various rock types. (A) Massive brown epidote in a vein in the Granite Mountain batholith (sample GBR2-14); field of view (F.o.V.) 1.13 × 1.50 mm. (B) Coarse, olive-green, euhedral bladed epidote in zeolite in a vein in the Mount Polley Intrusive Complex (sample 18PMA007); F.o.V. 1.13 × 1.50 mm. (C) Coarse yellow-green euhedral epidote with sulfides and magnetite in a vein in the Mount Polley Intrusive Complex (sample 18PMA009); F.o.V. 1.05 × 1.43 mm. (D) Pale yellow-green, fractured anhedral epidote intergrown with pyrite, titanite, and quartz (sample 13CDBWJ20); F.o.V. 1.08 × 1.45 mm. (E) Epidote and titanite replacing chlorite-altered biotite from the Granite Mountain batholith (sample 14PSCAP3); F.o.V. 1.10 × 1.47 mm. (F) Fine-grained poikilitic epidote in feldspar from the Granite Mountain batholith (sample GSC-1); F.o.V. 1.02 × 1.36 mm. (G) Fine-grained poikilitic epidote overprinting feldspar in the Mount Polley Intrusive Complex (sample 18PMA010); F.o.V 1.02 × 1.36 mm; PPL. (H) Subhedral epidote intergrown with carbonate and chlorite in metamorphosed Nicola Group pyroclastic rock (sample 16PSC12); F.o.V. 1.07 × 1.43 mm. (I) Poikilitic epidote overprinting chlorite and carbonate in Nicola Group volcanic rock. Fine hematite inclusions are present (sample 14PSC357); F.o.V. 1.02 × 1.36 mm. Cb = carbonate mineral, Chl = chlorite, Ep = epidote, Hem = hematite, Mag = magnetite, Pl = plagioclase, Py = pyrite, Qz = quartz, Sul = sulfides, Ttn = titanite, Zeo = zeolite.

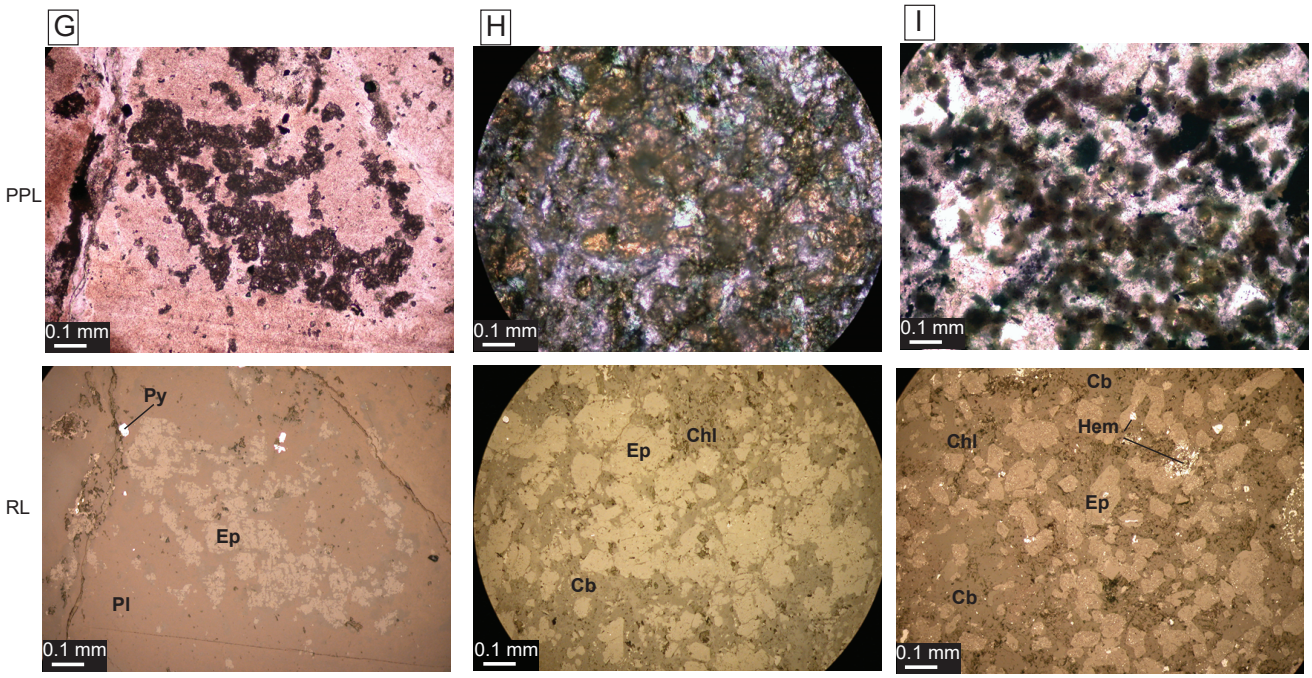

Fig. 4. *(Cont.)*

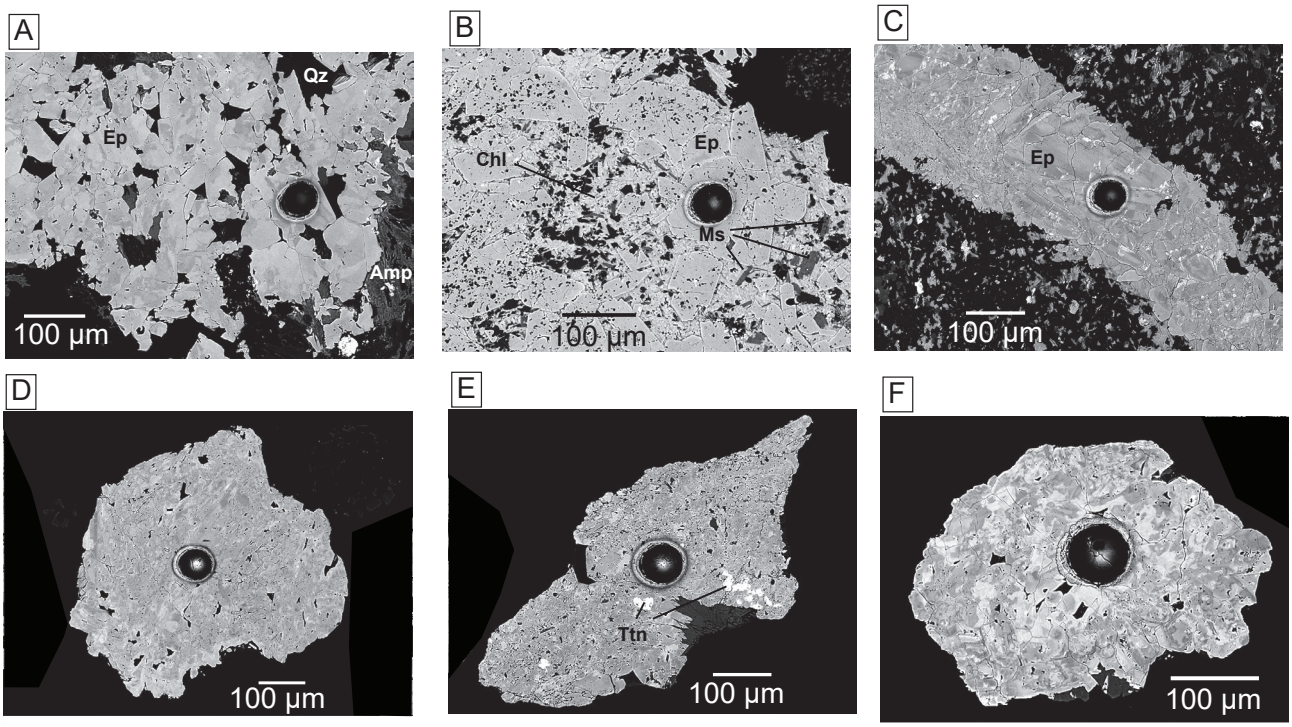

Fig. 5. Scanning electron microscope backscattered electron images of epidote in various rock samples. (A) Strong Fe-Al zoning in vein epidote in the intrusive rocks at Woodjam (sample 13CDBWJ22); Fe-rich areas (approximately 12 wt % Fe and 12 wt % Al) are brighter than Al-rich areas (approximately 10 wt % Fe and 13 wt % Al). (B) Euhedral epidote overprinting a pyroclastic fragment in Nicola Group rock (sample 17PSC134). (C) A veinlet of epidote in a fine-grained Nicola Group volcanic rock collected <1 km from the Granite Mountain batholith (sample GBR-49); note the Fe-Al zoning and the bright specks enriched in rare earth elements (0.9–1.1 wt % Nd; 0.7–1.1 wt % Ce). (D) An epidote grain from till sample 11PMA029 collected near (<1 km) the Gibraltar deposit. (E, F) Epidote grains from till sample 12PMA095 collected approximately 4 km northwest (down-ice) of the Mount Polley deposit. The black circles are laser ablation pits (50 µm). Amp = amphibole, Chl = chlorite, Ep = epidote, Ms = muscovite, Qz = quartz, Ttn = titanite.

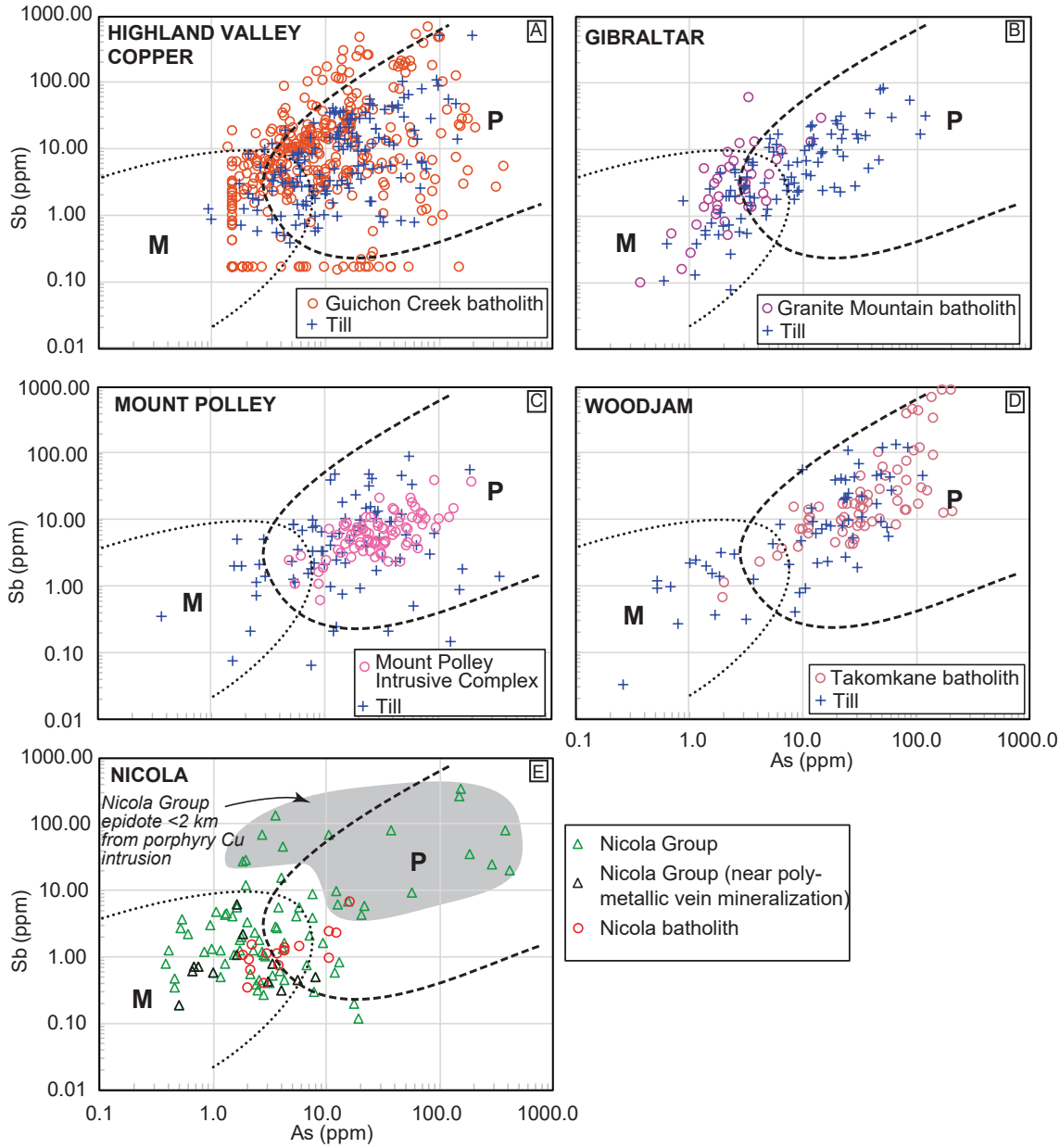

Fig. 6. Plots of As versus Sb for intrusive bedrock and till samples from (A) Highland Valley Copper, (B) Gibraltar, (C) Mount Polley, and (D) Woodjam. (E) The same plot showing Nicola Group and Nicola batholith bedrock samples. The black dotted and dashed lines define the approximate range of concentrations in metamorphic (M) and porphyry-alteration (P) epidote, respectively, as reported by Wilkinson et al. (2020) and Cooke et al. (2020b). Concentrations below detection limit are plotted using data not filtered for mean detection limit and are shown for illustration purposes.

in till classified as porphyry related, metamorphic, or uncertain is shown in Figure 8A, D, G, and J. Epidote grains classified as uncertain have a composition that falls in the overlapping area between porphyry and metamorphic fields in Figure 6. Till samples in which more than 50% of the epidote grains have a porphyry signature occur in each district but have no clear distribution patterns (Fig. 8A, D, G, J). However, five samples collected close to the mineralization at Mount Polley and two collected at Woodjam contain epidote grains that plot solely within the porphyry field (Fig. 8G, J).

The trace elements Mn, Cu, Zn, Sn, and Pb are also abundant in porphyry-related epidote (Cooke et al., 2014, 2020a, b; Jago et al., 2014; Byrne, 2019; Baker et al., 2020; Wilkinson et al., 2020) and, therefore, have the potential to indicate the source of this mineral. The concentrations of these elements in epidote are variable among the four porphyry study sites and, in some cases, are highly skewed from a normal distribution (e.g., Cu and Zn; Fig. 7). Sixty-seven percent of epidote from the bedrock samples from the Highland Valley Copper deposit returned Cu concentrations below the detection limit, and 57% of the epidote grains from the till returned Cu concentrations below the detection limit, with 36% below the detection limit for Sn. The highest concentrations of Mn, Cu, Zn, and Pb occur in epidote from porphyry-related intrusive

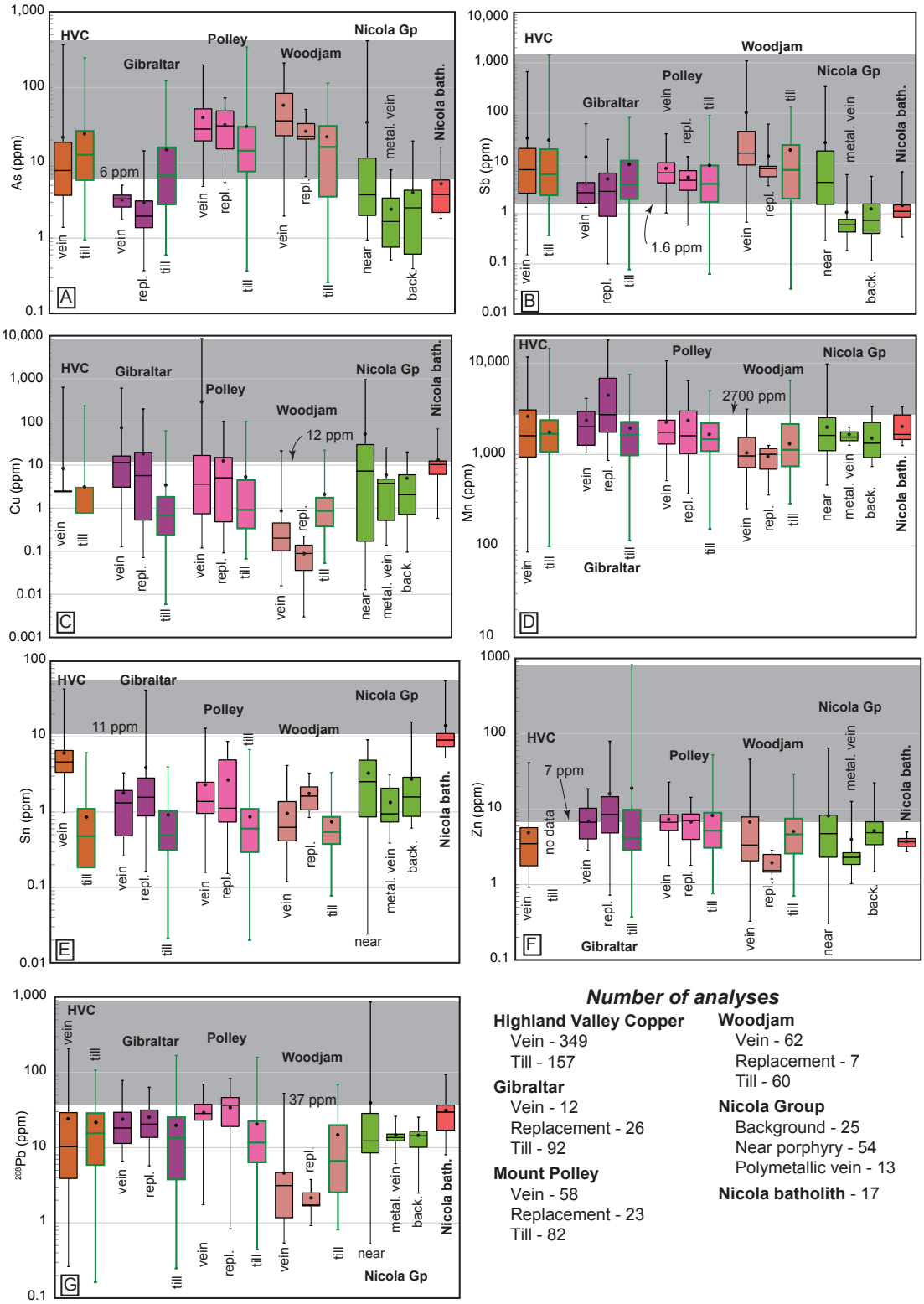

Fig. 7. Box and whisker plots of elemental concentrations in epidote: (A) As, (B) Sb, (C) Cu, (D) Mn, (E) Sn, (F) Zn, and (G) Pb. The box defines the first, second, and third quartile and the dot the mean concentration. The whiskers show the full ranges of concentration. Statistics were calculated with data not filtered for detection limit. Data are shown for vein epidote (vein), replacement epidote (repl.), and epidote grains from till (till). Epidote in Nicola Group rocks are classified as background metamorphic epidote (back.), epidote from near (<2 km) porphyry mineralization or intrusion with porphyry mineralization (near), and epidote from near polymetallic vein mineralization (metal. vein). The gray zone defines concentrations above a threshold defined as the highest third-quartile value in the background Nicola Group or the Nicola batholith. HVC = Highland Valley Copper, Nicola bath. = Nicola batholith.

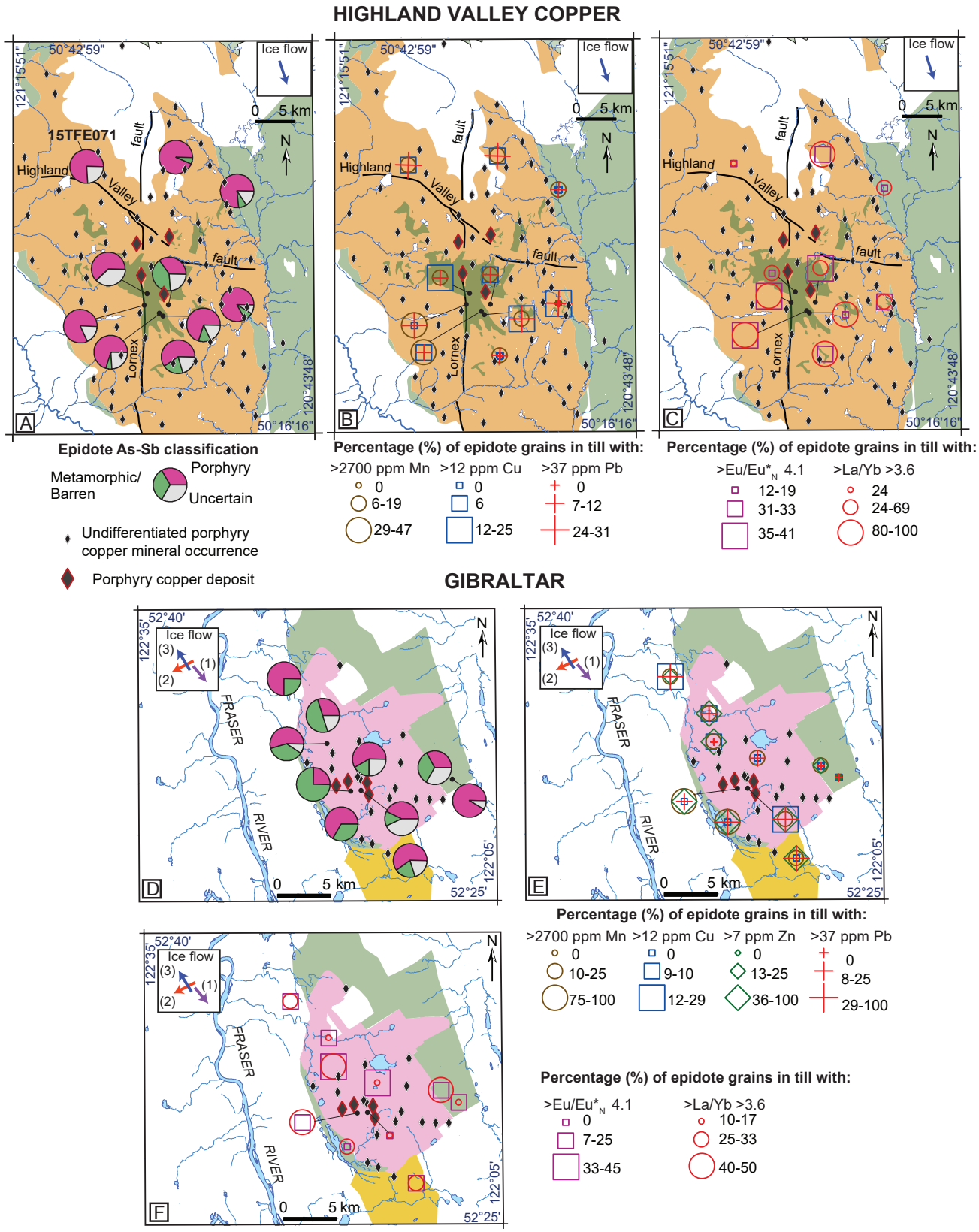

Fig. 8. Classification of epidote grains in till based on their As and Sb content (porphyry-related, metamorphic, or uncertain; see Fig. 6) and percentage of epidote grains in till with high trace element concentrations (>2,700 ppm Mn, >12 ppm Cu, >7 ppm Zn, >37 ppm Pb) and high rare earth element (REE) ratios (>4.1 Eu/Eu*$_N$, >3.6 La/Yb) at Highland Valley Copper (A, B, C), Gibraltar (D, E, F), Mount Polley (G, H, I), and Woodjam (J, K, L). On average, 11 epidote grains were analyzed per till sample. See Figure 2 for bedrock legend.

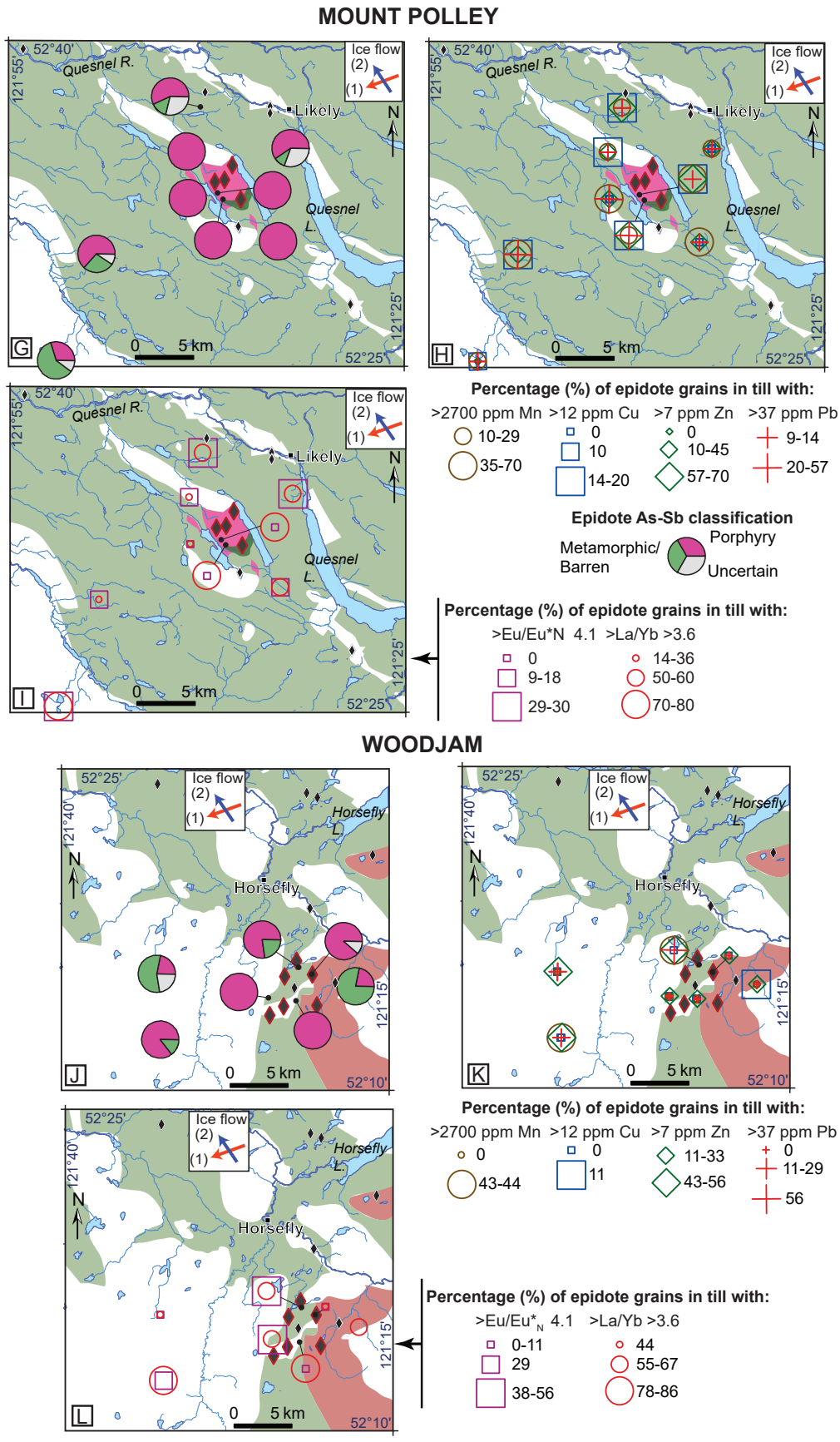

Fig. 8. *(Cont.)*

rocks from all four of the porphyry study sites and from Nicola Group rocks collected near mineralization (Fig. 7). Elevated concentrations of these trace elements are generally observed in both vein and replacement epidote (Fig. 7; see also Cooke et al., 2014; Ahmed et al., 2020). However, at Woodjam, higher Cu, Pb, and Zn concentrations are present in epidote veins compared to replacement epidote. Conversely, at Gibraltar, Mn concentrations are higher in replacement epidote.

To show the location of the till samples with epidote grains that contain the highest concentrations of these trace elements, an approximate threshold for each element was assigned to the highest third-quartile value in metamorphosed Nicola Group (background) or Nicola batholith samples, as both rock types are considered barren of mineralization (shaded band in Fig. 7). Concentrations above this threshold correspond to >2,700 ppm Mn, >12 ppm Cu, >7 ppm Zn, and >37 ppm Pb, and potentially indicate porphyry mineralization; the percentages of epidote grains from each till sample with concentrations above these thresholds are plotted (Fig. 8B, E, H, K). At Highland Valley Copper, the highest percentages of epidote grains with Mn, Cu, and/or Pb concentrations above this threshold occur in all but three of the till samples: one to the northeast over barren Nicola Group bedrock, one in the central part of the Guichon Creek batholith, and one in the south-central part of the batholith 7 km south of mineralization (Fig. 8B). Similarly, most till samples from Gibraltar and Mount Polley contain the highest percentages of epidote with elevated concentrations of at least one of these four trace elements (Fig. 8E, H). At Gibraltar, there are three exceptions: two samples collected to the east (up-ice of mineralization) over Nicola Group bedrock and one collected in the central part of the Granite Mountain batholith, <2 km north of mineralization (Fig. 8E). At Mount Polley, only two samples yielded low percentages of epidote with low concentrations of trace elements: one north of Quesnel Lake and the second in the southwest, both in background regions without known mineralization (Fig. 8H). At Woodjam, three samples collected near mineralization contained low percentages of epidote grains with anomalous Mn, Cu, Zn, and Pb concentrations (Fig. 8K).

The REE patterns of epidote from each rock type show several common trends and a few exceptions. The median REE concentrations (normalized to chondrites; McDonough and Sun, 1995) in epidote from intrusive rocks that host mineralization show the following general characteristics: concave to flat REE patterns with an average enrichment of 10× chondritic values, except for some light REE (LREE) enrichment (La/Yb_N ranges from 1.7 to 14.4) and positive Eu anomalies ($Eu/Eu^*_N = Eu_N/\sqrt{Sm_N \times Gd_N}$) that range from 1.7 in veins at Woodjam to a maximum of 6.0 in veins at Gibraltar (Fig. 9A, D, G, J). There are no consistent differences in the median REE patterns between the vein and replacement epidote. For example, the median Eu/Eu^*_N value is higher in the epidote from the veins at the Gibraltar deposit but is higher in the replacement epidote at Woodjam. Epidote from the barren Nicola batholith yielded a La/Yb_N value of 2.2 and a median Eu/Eu^*_N value of 2.3, both within the lower range observed in the porphyry-related intrusions (Fig. 9N). In contrast, epidote from the Nicola Group rocks all have lower median La/Yb_N (0.5–1.1) and generally lower Eu/Eu^*_N (1.6–1.8) values compared to epidote from porphyry-related intrusive rocks (Fig. 9M, N). The slightly higher Eu/Eu^*_N and La/Yb values in porphyry-related epidote are depicted with box and whisker plots (Fig. 10). There are exceptions to the general epidote REE trends described above; a limited number of epidote grains from the Guichon Creek batholith (40 of 349), Granite Mountain batholith (5 of 38), the Mount Polley Intrusive Complex (2 of 81), the Takomkane batholith (8 of 69), the Nicola Group (17 of 92), and the Nicola batholith (1 of 17) present negative Eu anomalies (App. Table A2). These commonly have convex LREE ($La_N < Ce_N$) patterns and overall stronger REE enrichment compared to epidote with positive Eu anomalies.

Epidote grains in till have a range of REE concentrations with patterns that reflect those observed in all rock types (Fig. 9). The median REE trend of the combined epidote population within each till sample indicates that there are generally elevated LREEs ($La/Yb_N > 1.7$) and $Eu/Eu^*_N > 1.7$ (Fig. 9B, E, H, K) in the epidote grains from till. Using the same approach as for trace elements—i.e., mapping the distribution of high percentages of epidote grains in till with greater than threshold Eu/Eu^*_N (4.1) and La/Yb (3.6) values (Fig. 10)—no distribution patterns could be linked to mineralization except for the highest percentages of grains, which have Eu/Eu^*_N values of >4.1 near mineralization at Highland Valley Copper, Gibraltar, and Woodjam (Fig. 8C, F, L).

Discussion

Using the optical or the MLA-SEM methods to determining the abundance of epidote in the heavy mineral concentrates of the till samples in the region of a prospective intrusion is the first step to detecting epidote that may be associated with a buried porphyry deposit, derived from either propylitic or sodic-calcic alteration (so-called "green rock" alteration; Cooke et al., 2014). Epidote dispersal trains in till, which can vary from 8 to 330 km^2 (Fig. 3), delineate a viable exploration target. Reconnaissance-level surveys with a till sample spacing of approximately 1 to 2 km (corresponding to one sample per 1–4 km^2), as was used in this study, is an efficient method to evaluate the regional mineralization potential of a covered prospective intrusion.

The Fe-Al irregular zoning observed in BSE images of porphyry-related epidote (Fig. 5A, C-F) can result from changes in redox conditions, temperature, pH, bulk-rock and fluid compositions, CO_2 fugacity, and, to a lesser extent, pressure (Holdaway, 1972; Arnason et al., 1993). The Fe-Al zoning suggests rapidly evolving physicochemical conditions during precipitation of the epidote from the hydrothermal fluids. The Fe-Al zoning is not well-developed in epidote from the Nicola Group metamorphosed rocks. However, irregular, oscillatory, and sector zoning, controlled by trace element composition, has been reported in metamorphic epidote elsewhere (Franz and Liebscher, 2004; Grapes and Hoskin, 2004). Therefore, the presence of Fe-Al zoning in epidote is not a clear indication of a porphyry provenance.

The concentrations of trace elements (Mn, Cu, Zn, As, Sb, Pb) in epidote that were determined by LA-ICP-MS may provide additional confirmation that the epidote is related to porphyry mineralization. In this study, the As and Sb contents in the epidote appear to be the most consistent indicator of porphyry mineralization, except at Gibraltar, where low As concentrations in the epidote could be related to its

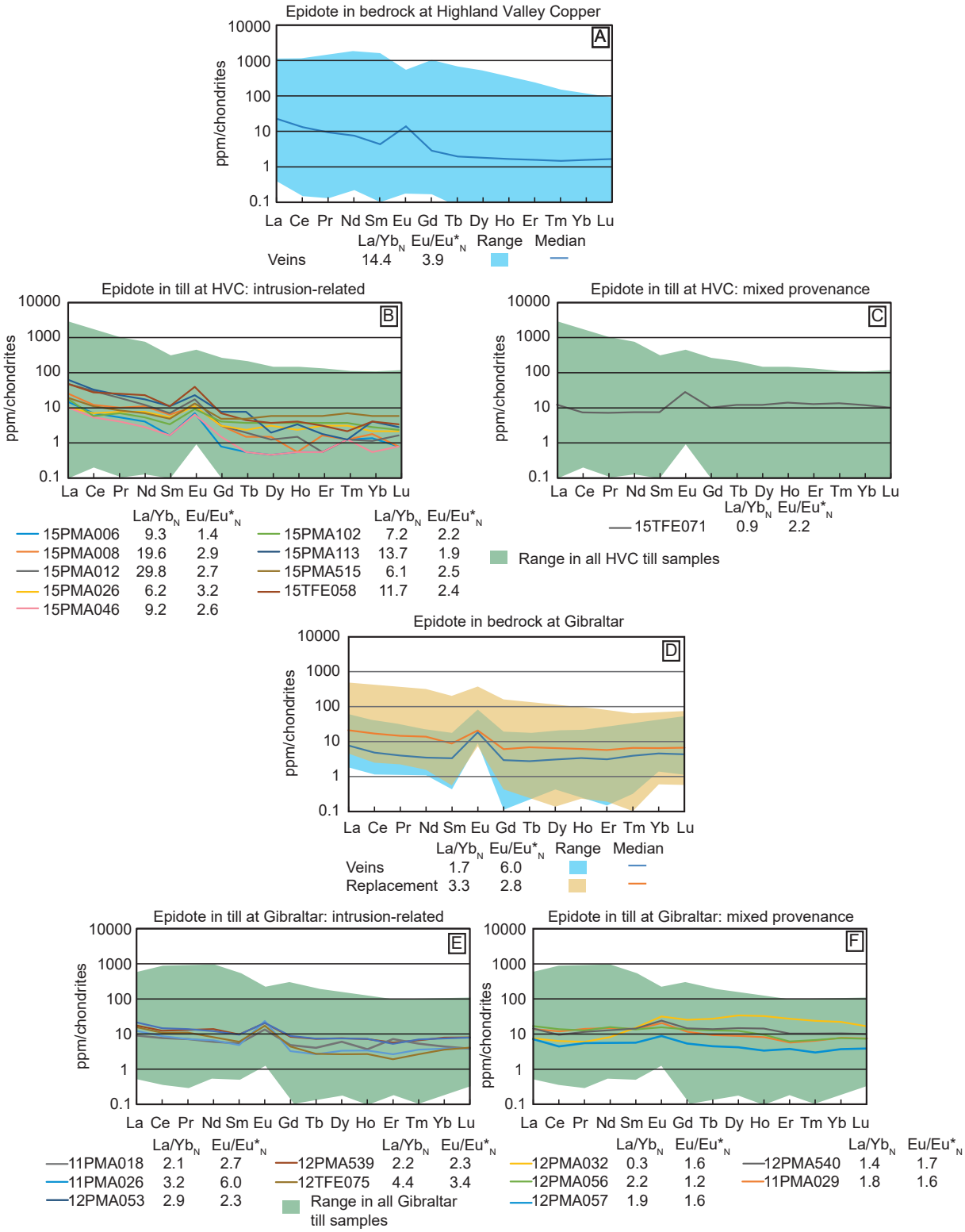

Fig. 9. Median rare earth element (REE) concentrations (ppm) normalized to chondrite values (McDonough and Sun, 1995) for epidote from the (A, B, C) Highland Valley Copper, (D, E, F) Gibraltar, (G, H, I) Mount Polley, and (J, K, L) Woodjam deposits. The results are shown for bedrock and till samples and indicate two groups of epidote: those dominantly from intrusive rocks and those with mixed provenance. The lines in the graphs are constructed from the median REE concentrations; the shaded areas represent the full range of concentrations. (M, N) Epidote REE concentrations from Nicola Group and Nicola batholith samples. La/Yb and Eu/Eu*$_N$ calculated from the median concentrations, depicted as lines on the REE plots, are provided below each graph. HVC = Highland Valley Copper, Near poly vein = near polymetallic vein mineralization, Near porph. = near porphyry mineralization, Nicola bath. = Nicola batholith.

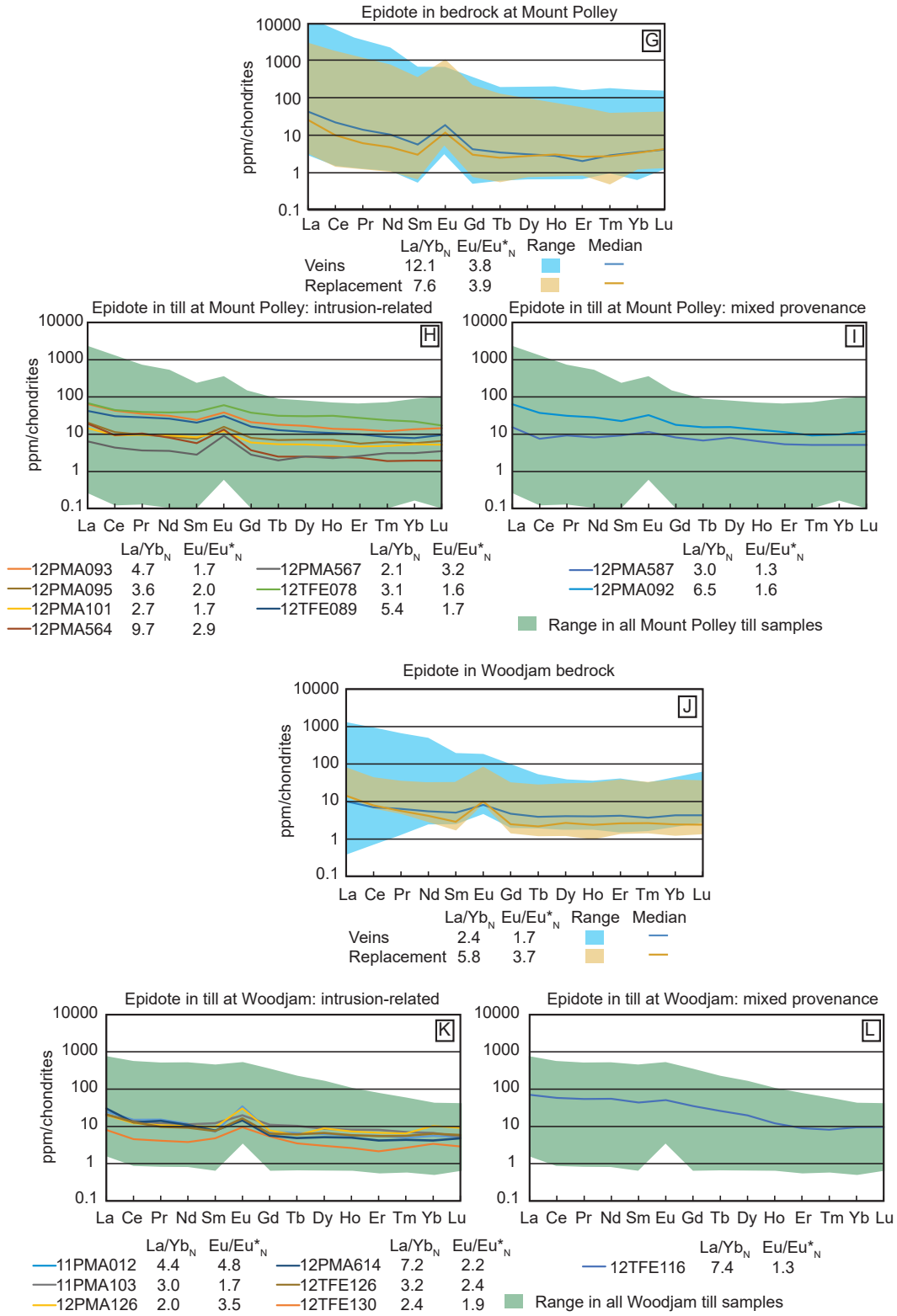

Fig. 9. *(Cont.)*

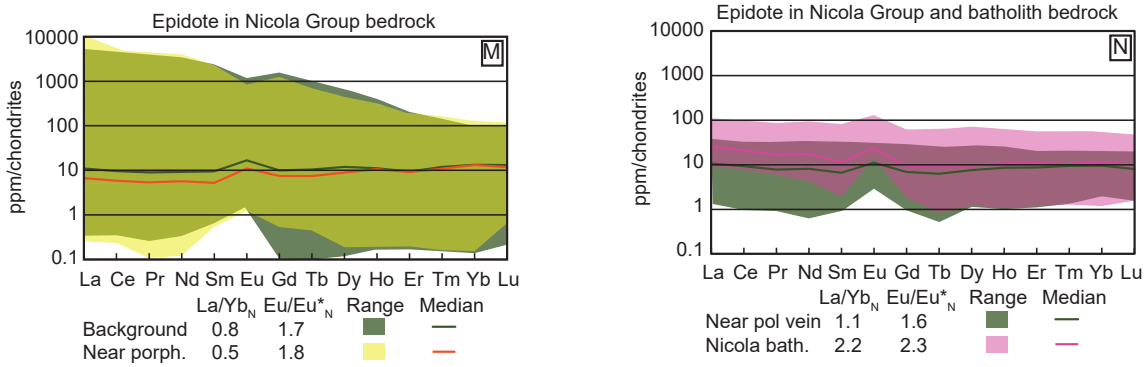

Fig. 9. *(Cont.)*

recrystallization during postmineralization metamorphism (Plouffe et al., 2021a, 2022). High concentrations of one or both of these elements are encountered in the majority of the epidote grains from till from each of the four study sites. We interpret the regional distribution of epidote in till with high As and Sb (>8 ppm As and >0.6 ppm Sb; Fig. 6) to be derived from porphyry hydrothermal alteration zones. Till epidote grains with low As and Sb concentrations are most likely derived from the metamorphosed Nicola Group rocks distal (>2 km) from mineralization or from other barren rocks.

High percentages of epidote grains in till with high concentrations of trace elements (>2,700 ppm Mn, >12 ppm Cu, >7 ppm Zn, and >37 ppm Pb, i.e., threshold values) are heterogeneously distributed in each of the porphyry districts and are less abundant in background regions where mineralization is absent. No clear regional dispersal patterns of detrital epidote with proximal (Cu) and distal (Mn, Zn, Pb) trace element signatures are associated with the main mineralized zones. Epidote grains with high concentrations of pathfinder elements in till samples collected >10 km southwest of Mount Polley and west-southwest of Woodjam could be derived from the known mineralization and transported to the southwest during the first phase of ice flow; alternatively, this epidote may be derived from an unknown source. Some till samples collected near mineralization that have high percentages of porphyry-related epidote grains, based on their As and Sb concentrations, contain low percentages of grains with high concentrations of the trace elements Mn, Cu, Zn, and Pb (Fig. 8). In other words, the high concentrations of Mn, Cu, Zn, and Pb in the epidote grains are not as consistent an indicator of porphyry mineralization as high As and Sb concentrations.

The variability in the abundance of epidote grains in the till samples that may have been derived from porphyry mineralization and the inconsistent spatial patterns for these epidote grains to be enriched in pathfinder elements (proximal Cu and distal Mn, Zn, As, Sb, and Pb) are interpreted to be related to a combination of factors: (1) the variable composition of the epidote in the bedrock with increasing distance from multiple mineralization centers within the broader porphyry district, as previously reported (Cooke et al., 2014, 2020a, b; Byrne, 2019; Baker et al., 2020; Wilkinson et al., 2020), (2) the mixed provenance of the epidote grains in till, and (3) trace element zoning within epidote (Fig. 11; see also Ahmed et al., 2020). Indeed, detailed LA-ICP-MS mapping of the epidote shows that the trace elements are heterogeneously distributed within the mineral structure, with zoning patterns partly mimicking the Fe-Al distribution (Fig. 11A; Plouffe et al., 2023). In the case of Cu, it appears to be a late addition to

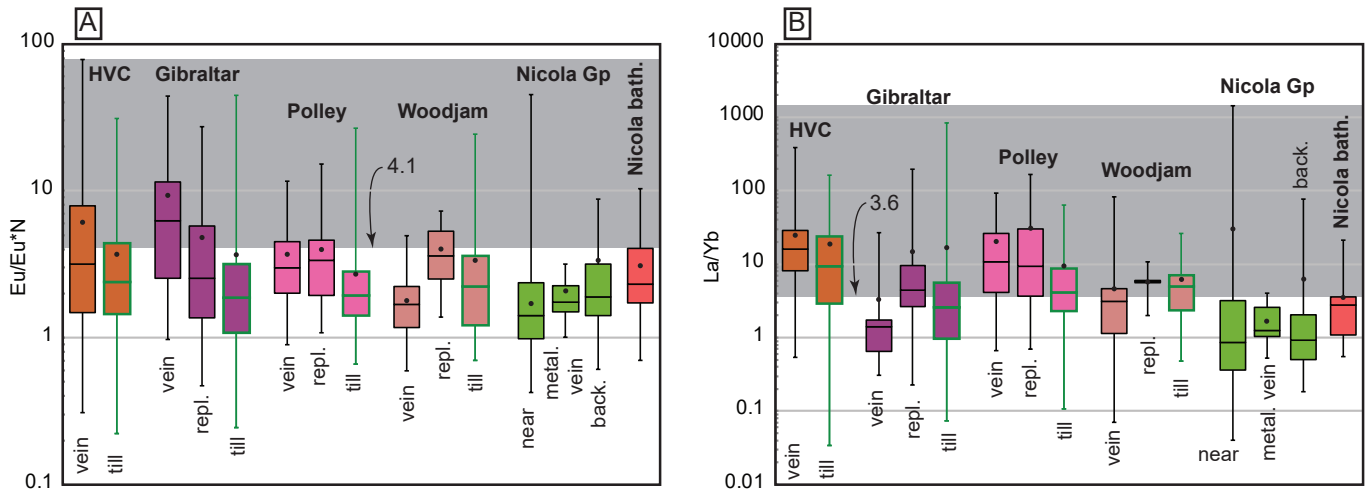

Fig. 10. Box and whisker plots of (A) Eu/Eu*$_N$ and (B) La/Yb in epidote. The format and abbreviations are the same as those in Figure 7. The gray zone defines concentrations above a threshold defined as the highest third-quartile value in the background Nicola Group or the Nicola batholith rocks.

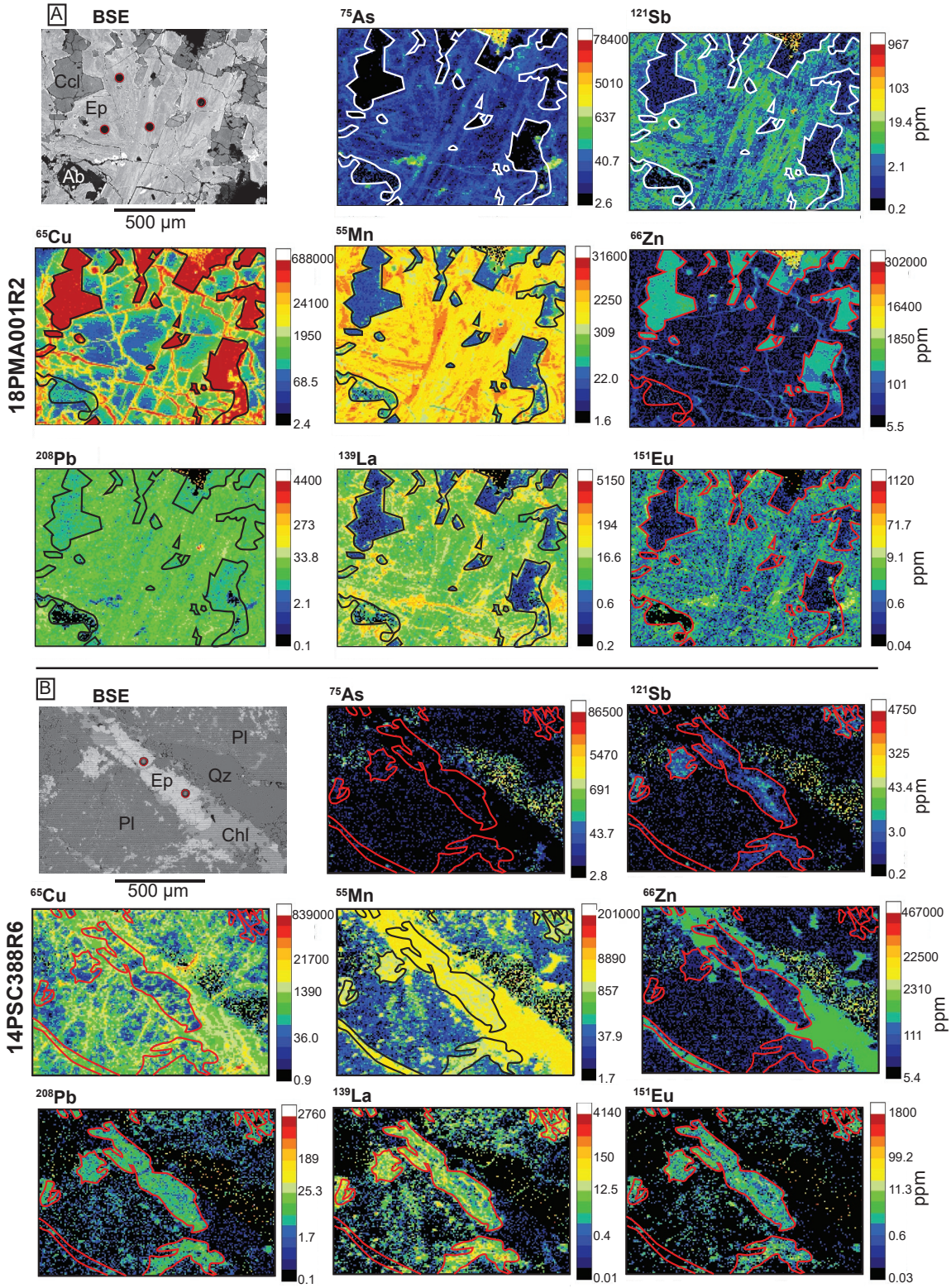

Fig. 11. Backscattered electron (BSE) images and laser ablation-inductively coupled plasma-mass spectrometry (LA-ICP-MS) maps of epidote. (A) The top nine images are of sample 18PMA001 from Mount Polley. Note the As, Sb, Mn, and Pb zoning that mimics the Fe-Al zoning (visible in the upper left BSE image) and the Cu, Zn, La, and Eu enrichments that occur along the fractures and the zoning in epidote. (B) The bottom nine images are of sample 14PSC388 from Gibraltar with epidote in a chlorite veinlet bordering quartz and altered plagioclase with fine-grained epidote. BSE image taken after LA-ICP-MS mapping. Note the poor ablation of quartz in the BSE image, the absence of As, Mn, Zn, and Pb zoning, higher Sb concentrations in the core, higher La and Eu concentrations in the rim, and net-textured Cu concentrations infiltrating along grain boundaries.

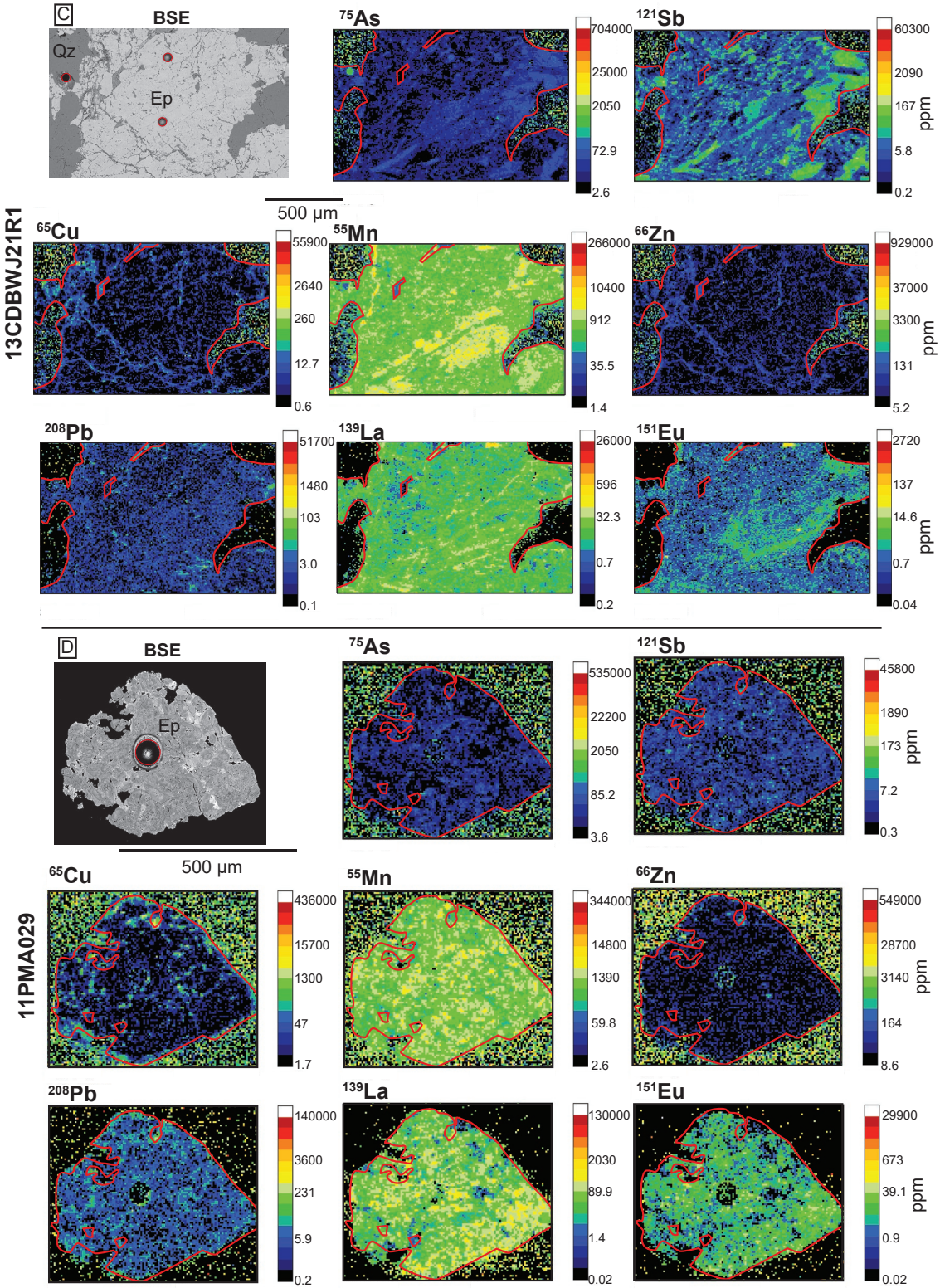

Fig. 11. *(Cont.)* (C) The top nine images are of sample 13CDBWJ21 from Woodjam. Note that As, Sb, Mn, La, and Eu zoning all have a similar orientation but that the highest concentrations occur in different locations within the epidote. The higher concentrations of Cu and Zn along the fractures in the epidote suggest a late addition of these metals by hydrothermal fluids after the epidote was formed. The laser pit in quartz was not included in the assessment of the epidote composition. (D) The bottom nine images are of an epidote grain from till sample 11PMA029 collected in the region of the Gibraltar deposit. Note the Fe-Al zoning visible in the BSE image. The high concentrations of Cu, La, and Eu follow the high Fe zoning (bright regions in the BSE image), low concentrations of As, Sb, and Zn, and heterogeneous distribution of Mn and Pb. On all BSE images, the red circles are laser pits. Ab = albite, Ccl = chrysocolla, Chl = chlorite, Ep = epidote, Pl = plagioclase, Qz = quartz.

the epidote, as it is abundant along the grain boundaries and fractures (Fig. 11A-C). Consequently, the heterogeneous distribution of pathfinder elements in the epidote accounts for some of the variability observed in compositions determined by LA-ICP-MS spot analyses. To evaluate porphyry mineralization potential, a large number of epidote grains from each till sample should be analyzed to compensate for the heterogeneous distribution of these pathfinder elements.

In this study, analyzing an average of 11 randomly selected grains per till sample, in seven to 10 till samples in each district, indicated a possible porphyry signal. Multiple analyses of each epidote grain should be conducted, where possible, to account for possible growth zoning. The epidote grains from till in this study commonly contained fractures and inclusions and were commonly intergrown with other minerals, limiting the ability to use multiple laser spots.

Rare earth elements provide only a vague indication of the provenance of detrital epidote. The ratio $La/Yb_N > 1.7$, as measured in epidote from intrusive rocks in this study and in felsic to intermediate igneous rocks in other studies (e.g., Frei et al., 2004; Anenburg et al., 2015), is interpreted to reflect a provenance of felsic to intermediate granitoids and does not indicate a porphyry Cu provenance. Enrichment of LREEs in epidote could be related to the large ionic radii of LREEs, which are better accommodated in the large Ca^{2+} cation site available in epidote (cf. Gieré and Sorensen, 2004) and the greater solubility of LREEs in F- and Cl-bearing fluids at temperatures <300°C (Migdisov et al., 2009). An Eu/Eu^*_N value of >4.1 measured in epidote from porphyry-related intrusive rocks (Fig. 10) could be diagnostic of a porphyry source. However, elevated Eu/Eu^*_N in epidote from till provides only a vague indication of the presence of mineralization. Till samples with the highest percentages of grains with Eu/Eu^*_N values >4.1 were from sample sites close to the mineralization at Highland Valley Copper, Gibraltar, and Woodjam; however, at Mount Polley, epidote with elevated Eu/Eu^*_N values was found in barren rocks southwest and northeast of the mine (Fig. 8). The origin of the epidote with positive Eu/Eu^*_N anomalies is unclear. It is possible that this enrichment is an inheritance from the primary Ca-bearing mineral (e.g., plagioclase) that was replaced by epidote, as has been observed in metamorphic rocks (El Korh, et al., 2009). Additionally, the preferential incorporation of Eu^{3+} in epidote as it crystallizes from oxidized hydrothermal fluids might contribute to the positive Eu anomaly. Due to similar radii, Eu^{3+} (atomic radius = 1.03 Å) can replace Ca^{2+} (atomic radius = 1.00 Å) in the A sites with concomitant replacement of trivalent for divalent cation in the M sites to maintain charge balance (Frei et al., 2004). More studies of the REE composition of epidote are required before it can be stated that the enrichment is related to porphyry Cu mineralization and hydrothermal alteration.

Using the composition of epidote as an indicator of provenance is not unique to mineral exploration. Epidote is recognized as a provenance indicator in sedimentary basins based on its Nd and Sr isotope and trace element composition, which has implications for the exhumation history of the Central Alps (e.g., Spiegel et al., 2002). Identifying the presence of detrital minerals associated with porphyry hydrothermal alteration, such as epidote, can be useful as part of a mineral exploration strategy in places where mineralization is deeply seated and has not undergone glacial erosion. In such cases, direct indicators of porphyry Cu mineralization, such as chalcopyrite grains or Cu geochemical anomalies (cf. Plouffe et al., 2016, 2022), would be absent, and only resistant minerals associated with the alteration zones, such as epidote, would be present in the till. Hence, recognizing the potential for porphyry Cu mineralization based on the presence of porphyry alteration minerals (e.g., apatite, tourmaline) and even igneous minerals (e.g., zircon) can contribute to the discovery of deeper porphyry mineralization buried under sediment cover (Mao et al., 2016, 2017; Lee et al., 2021; Plouffe et al., 2021a; Beckett-Brown et al., 2023a, b). Once a potential porphyry Cu source has been identified using the abundance and composition of detrital epidote, vectoring toward mineralization could be achieved using bedrock samples of epidote (and chlorite) as shown by Cooke et al. (2020b) and Wilkinson et al. (2020).

Conclusion

The abundance and composition of detrital epidote from till (glacial sediment) can be used in mineral exploration to detect propylitic and/or sodic-calcic alteration associated with porphyry Cu deposits. In the Quesnel terrane of the Canadian Cordillera, epidote was found to be more abundant in the heavy mineral concentrates from till collected over and downice of four porphyry Cu deposits (Highland Valley Copper, Gibraltar, Mount Polley, Woodjam) than in till from the surrounding regions that are barren of mineralization. The composition of epidote, particularly elevated As (>8 ppm) and Sb (>0.6 ppm) content, is useful to differentiate detrital epidote grains derived from porphyry alteration versus regional metamorphic rocks of the Nicola Group. In addition, high abundance and heterogeneous distribution of epidote grains in till with high concentrations of trace elements (>12 ppm Cu, >2,700 ppm Mn, >7 ppm Zn, and >37 ppm Pb) provide an indication that an intrusion might host porphyry Cu ore. This signal was not observed in regions that are barren of known mineralization. Tracing detrital epidote in glaciated terrains may be particularly applicable if a mineralized zone is at depth and only the nonmineralized propylitic or sodic-calcic alteration zones that contain epidote were exposed to glacial erosion. This mineral exploration method can be further tested and developed to aid the discovery of the next generation of porphyry Cu deposits that are needed to meet the demands for this critical mineral (Natural Resources Canada, 2021).

Acknowledgments

The first author dedicates this paper to R.G. Anderson, with whom the idea of investigating the abundance and composition of epidote in till as a mean of conducting mineral exploration in the Quesnel terrane was first entertained in the fall of 2011 while having lunch on a "green rock" altered outcrop of the Granite Mountain batholith. This research greatly benefited from samples provided by J.B. Chapman, C.H. Kobylinski, C. Rees, and P. Schiarizza. Marghaleray Amini from the PCIGR-UBC and Pat Hunt and Matthew Polivchuk from the GSC are acknowledged for their laboratory support. The authors acknowledge and appreciate the direct and indirect support provided by the mine operators and exploration site owners: Teck Resources Limited (Highland Valley Copper), Taseko Mines Limited (Gibraltar), Imperial Metals

Corporation (Mount Polley), and Consolidated Woodjam Copper (Woodjam). This study was supported by the Targeted Geoscience Initiative of the Geological Survey of Canada, the Natural Sciences and Engineering Research Council of Canada (NSERC), and the Canadian Mining Innovation Council (CMIC) Mineral Exploration Footprints project at Highland Valley Copper. The paper benefited from reviews by C.E. Beckett-Brown (GSC internal review), and two journal reviewers: J. Hedenquist and one anonymous reviewer. This is Natural Resources Canada contribution 20220149 and NSERC-CMIC contribution 232.

REFERENCES

Ahmed, A.D., Fisher, L., Pearce, M., Escolme, A., Cooke, D.R., Howard, D., and Belousov, I., 2020, A microscale analysis of hydrothermal epidote: Implications for the use of laser ablation-inductively coupled plasma-mass spectrometry mineral chemistry in complex alteration environments: Economic Geology, v. 115, p. 793–811.

Anenburg, M., Katzir, Y., Rhede, D., Jöns, N., and Bach, W., 2015, Rare earth element evolution and migration in plagiogranites: A record preserved in epidote and allanite of the Troodos ophiolite: Contributions to Mineralogy and Petrology, v. 169, 25 p.

Armbruster, T., Bonazzi, P., Akasaka, M., Bermanec, V., Chopin, C., Gieré, R., Heuss-Assbichler, S., Liebscher, A., Menchetti, S., Pan, Y., and Pasero, M., 2006, Recommended nomenclature of epidote-group minerals: European Journal of Mineralogy, v. 18, p. 551–567.

Arnason, J.G., Bird, D.K., and Liou, J.G., 1993, Variables controlling epidote composition in hydrothermal and low-pressure regional metamorphic rocks: 125 Years Knappenwand, Salzburg, Austria, 1993, Symposium Proceedings, p. 17–25.

Arnold, H., and Ferbey, T., 2020, Ice-flow indicator database, British Columbia and Yukon: British Columbia Ministry of Energy and Mines and Petroleum Resources, British Columbia Geological Survey, Open File 2020-03, 1 p.

Arnold, H., Ferbey, T., and Hickin, A.S., 2016, Ice-flow indicator compilation, British Columbia and Yukon: Geological Survey of Canada, Open File 8083, and British Columbia Geological Survey, Open File 2016-04, scale 1:1,750,000.

Ash, C.H., and Riveros, C.P., 2001, Geology of the Gibraltar copper-molybdenite deposit, east-central British Columbia (93B/9): British Columbia Ministry of Energy and Mines, Geological Fieldwork 2000, Paper 2001-1, p. 119–134.

Baker, M.J., Wilkinson, J.J., Wilkinson, C.C., Cooke, D.R., and Ireland, T., 2020, Epidote trace element chemistry as an exploration tool in the Collahuasi district, northern Chile: Economic Geology, v. 115, p. 749–770.

Beckett-Brown, C.E., McDonald, A.M., and McClenaghan, M.B., 2023a, Recognizing tourmaline in mineralized porphyry Cu systems: Textures and major-element chemistry: The Canadian Journal of Mineralogy and Petrology, v. 61, p. 3–29.

Beckett-Brown, C.E., McDonald, A.M., and McClenaghan, M.B., 2023b, Trace element characteristics of tourmaline in porphyry Cu systems: Development and application to discrimination: The Canadian Journal of Mineralogy and Petrology, v. 61, p. 31–60.

Berry, L.G., Mason, B., and Dietrich, R.V., 1983, Mineralogy: San Francisco, W.H. Freeman and Company, 561 p.

Bird, D.K., and Spieler, A.R., 2004, Epidote in geothermal systems: Reviews in Mineralogy and Geochemistry, v. 56, p. 235–300.

Bird, D.K., Schiffman, P., Elders, W.A., Williams, A.E., and McDowell, S.D., 1984, Calc-silicate mineralization in active geothermal systems: Economic Geology, v. 79, p. 671–695.

Bowman, J.R., Parry, W.T., Kropp, W.P., and Kruer, S.A., 1987, Chemical and isotopic evolution of hydrothermal solutions at Bingham, Utah: Economic Geology, v. 82, p. 395–428.

British Columbia Geological Survey, 2020, MINFILE British Columbia mineral deposits database: https://minfile.gov.bc.ca/, accesssed February 2020.

Byrne, K., 2019, Diagnostic features of the rocks and minerals peripheral to the Highland Valley Copper district, British Columbia, Canada: Implications for the genesis of porphyry Cu systems and their footprints: Ph.D. thesis, Edmonton, Canada, The University of Alberta, 211 p.

Byrne, K., Lesage, G., Gleeson, S.A., Piercey, S.J., Lypaczewski, P., and Kyser, K., 2020a, Linking mineralogy to lithogeochemistry in the Highland Valley Copper district: Implications for porphyry copper footprints: Economic Geology, v. 115, p. 871–901.

Byrne, K., Trumbull, R.B., Lesage, G., Gleeson, S.A., Ryan, J., Kyser, K., and Lee, R.G., 2020b, Mineralogical and isotopic characteristics of sodic-calcic alteration in the Highland Valley Copper district, British Columbia, Canada: Implications for fluid sources in porphyry Cu systems: Economic Geology, v. 115, p. 841–870.

Clague, J.J., and Ward, B.C., 2011, Pleistocene glaciation of British Columbia, *in* Ehlers, J., Gibbard, P.L., and Hughes, P.D., eds., Developments in Quaternary sciences, v. 15, Quaternary glaciations—extent and chronology a closer look: Amsterdam, Elsevier, p. 563–573.

Clarke, G., Northcote, B., Katay, F., and Tombe, S.P., 2021, Exploration and mining in British Columbia, 2020: A summary: British Columbia Geological Survey, Information Circular 2021-01, British Columbia Ministry of Energy, Mines and Low Carbon Innovation, p. 1–45.

Cooke, D.R., Baker, M., Hollings, P., Sweet, G., Zhaoshan, C., Danyushevsky, L., Gilbert, S., Zhou, T., White, N., Gemmell, J.B., and Inglis, S., 2014, New advances in detecting the distal geochemical footprints of porphyry systems—epidote mineral chemistry as a tool for vectoring and fertility assessments: Society of Economic Geologists, Special Publication 18, p. 127–152.

Cooke, D.R., Agnew, P., Hollings, P., Baker, M., Chang, Z., Wilkinson, J.J., Ahmed, A., White, N.C., Zhang, L., Thompson, J., et al., 2020a, Recent advances in the application of mineral chemistry to exploration for porphyry copper-gold-molybdenum deposits: Detecting the geochemical fingerprints and footprints of hypogene mineralization and alteration: Geochemistry: Exploration, Environment, Analysis, v. 20, p. 176–188.

Cooke, D.R., Wilkinson, J.J., Baker, M., Agnew, P., Phillips, J., Chang, Z., Chen, H., Wilkinson, C.C., Inglis, S., Hollings, P., Zhang, L., et al., 2020b, Using mineral chemistry to aid exploration: A case study from the Resolution porphyry Cu-Mo deposit, Arizona: Economic Geology, v. 115, p. 813–840.

Cui, Y., Miller, D., Schiarizza, P., and Diakow, L.J., 2017, British Columbia digital geology: British Columbia Ministry of Energy, Mines and Petroleum Resources, British Columbia Geological Survey, Open File 2017-8, 9 p.

D'Angelo, M., 2016, Geochemistry, petrography and mineral chemistry of the Guichon Creek and Nicola batholiths, southcentral British Columbia: M.Sc. thesis, Thunder Bay, Canada, Lakehead University, 421 p.

del Real, I., Bouzari, F., Rainbow, A., Bissig, T., Blackwell, J., Sherlock, R., Thompson, J.F.H., and Hart, C.J.R., 2017, Spatially and temporally associated porphyry deposits with distinct Cu/Au/Mo ratios, Woodjam district, central British Columbia: Economic Geology, v. 112, p. 1673–1717.

del Real, I., Bouzari, F., and Sherlock, R., 2020, The magmatic and hydrothermal evolution of the Woodjam Cu-Au and Cu-Mo porphyry district, central British Columbia, Canada: Canadian Institute of Mining, Metallurgy and Petroleum, Special Volume 57, p. 601–620.

Dyke, A.S., 2004, An outline of North American deglaciation with emphasis on central and northern Canada, *in* Ehlers, J., and Gibbard, P.L., eds., Quaternary glaciations—extent and chronology, part II: Amsterdam, Elsevier, p. 373–424.

El Korh, A., Schmidt, S.T., Ulianov, A., and Potel, S., 2009, Trace element partitioning in HP-LT metamorphic assemblages during subduction-related metamorphism, Ile de Groix, France: A detailed LA-ICPMS study: Journal of Petrology, v. 50, p. 1107–1148.

Erdmer, P., Moore, J.M., Heaman, L., Thomson, R.I., Daughtry, K.L., and Creaser, R.A., 2002, Extending the ancient margin outboard in the Canadian Cordillera: Record of Proterozoic crust and Paleocene regional metamorphism in the Nicola horst, southern British Columbia: Canadian Journal of Earth Sciences, v. 39, p. 1605–1623.

Ferbey, T., Plouffe, A., and Bustard, A.L., 2016, Geochemical, mineralogical, and textural data from tills in the Highland Valley Copper mine area, south-central British Columbia: British Columbia Geological Survey GeoFile 2016-11, Geological Survey of Canada Open File 8119, 15 p.

Franz, G., and Liebscher, A., 2004, Physical and chemical properties of the epidote minerals—an introduction: Reviews in Mineralogy and Geochemistry, v. 56, p. 1–82.

Fraser, T.M., Godwin, C.I., Thompson, J.F.H., and Stanley, C.R., 1993, Geology and alteration of the Mount Polley alkalic porphyry copper-gold deposit, British Columbia (93A/12): British Columbia Ministry of Energy, Mines and Petroleum Resources, Geological Fieldwork 1992, Paper 1993-1, p. 295–300.

Fraser, T.M., Stanley, C.R., Nikic, Z.T., Pesalj, R., and Gorc, D., 1995, The Mount Polley alkalic porphyry copper-gold deposit, south-central British Columbia: Canadian Institute of Mining and Metallurgy, Special Volume 46, p. 609–622.

Frei, D., Liebscher, A., Franz, G., and Dulski, P., 2004, Trace element geochemistry of epidote minerals: Reviews in Mineralogy and Geochemistry, v. 56, p. 553–605.

Gieré, R., and Sorensen, S.S., 2004, Allanite and other REE-rich epidote-group minerals: Reviews in Mineralogy and Geochemistry, v. 56, p. 431–493.

Grapes, R.H., and Hoskin, P.W.O., 2004, Epidote group minerals in low-medium pressure metamorphic terranes: Reviews in Mineralogy and Geochemistry, v. 56, p. 301–345.

Greenwood, H.J., Woodsworth, G.J., Read, P.B., Ghent, E.D., and Evenchick, C.A., 1991, Metamorphism, *in* Gabrielse, H., and Yorath, C.J., eds., Geology of the Cordilleran orogen in Canada, Geology of Canada, no. 4: Ottawa, Geological Survey of Canada, p. 535–570.

Hashmi, S., Ward, B.C., Plouffe, A., Leybourne, M.I., and Ferbey, T., 2015, Geochemical and mineralogical dispersal in till from the Mount Polley Cu-Au porphyry deposit, central British Columbia, Canada: Geochemistry: Exploration, Environment, Analysis, v. 15, p. 234–249.

Holdaway, M.J., 1972, Thermal stability of Al-Fe epidote as a function of f_{O_2} and Fe content: Contributions to Mineralogy and Petrology, v. 37, p. 307–340.

Jago, C.P., Tosdal, R.M., Cooke, D.R., and Harris, A.C., 2014, Vertical and lateral variation of mineralogy and chemistry in the Early Jurassic Mt. Milligan alkalic porphyry Au-Cu deposit, British Columbia, Canada: Economic Geology, v. 109, p. 1005–1033.

Kelley, K.D., Eppinger, R.G., Lang, J., Smith, S.M., and Fey, D.L., 2011, Porphyry Cu indicator minerals in till as an exploration tool: Example from the giant Pebble porphyry Cu-Au-Mo deposit, Alaska, USA: Geochemistry: Exploration, Environment, Analysis, v. 11, p. 321–334.

Kobylinski, C., Hattori, K., Plouffe, A., and Smith, S., 2017, Epidote associated with the porphyry Cu-Mo mineralization at the Gibraltar deposit, south central British Columbia: Geological Survey of Canada, Open File 8279, 19 p.

Lawley, C.J.M., Creaser, R., Jackson, S., Yang, Z., Davis, B., Pehrsson, S., Dubé, B., Mercier-Langevin, P., and Vaillancourt, D., 2015, Unravelling the Western Churchill province Paleoproterozoic gold metallotect: Constraints from Re-Os arsenopyrite and U-Pb xenotime geochronology and LA-ICP-MS arsenopyrite geochemistry at the BIF-hosted Meliadine gold district, Nunavut, Canada: Economic Geology, v. 110, p. 1425–1454.

Lawley, C.J.M., Petts, D.C., Jackson, S.E., Zagorevski, A., Pearson, D.G., Kjarsgaard, B.A., Savard, D., and Tschirhart, V., 2020, Precious metal mobility during serpentinization and breakdown of base metal sulphide: Lithos, v. 354–355, article 105278.

Lee, R.G., Plouffe, A., Ferbey, T., Hart, C.J.R., Hollings, P., and Gleeson, S.A., 2021, Recognizing porphyry copper potential from till zircon composition: A case study from the Highland Valley porphyry district, south-central British Columbia: Economic Geology, v. 116, p. 1035–1045.

Logan, J.M., and Mihalynuk, M.G., 2014, Tectonic controls on Early Mesozoic paired alkaline porphyry deposit belts (Cu-Au ± Ag-Pt-Pd-Mo) within the Canadian Cordillera: Economic Geology, v. 109, p. 827–858.

Logan, J.M., and Schroeter, T.G., eds., 2013, Porphyry systems of central and southern British Columbia: Tour of central British Columbia porphyry deposits from Prince George to Princeton: Society of Economic Geologists, Guidebook Series, v. 44, 143 p.

Logan, J.M., Schiarizza, P., Struik, L.C., Barnett, C., Nelson, J.L., Kowalczyk, P., Ferri, F., Mihalynuk, M.G., Thomas, M.D., Gammon, P., Lett, R., Jackaman, W., and Ferbey, T., (compilers), 2010, Bedrock geology of the QUEST map area, central British Columbia: Geoscience BC Report 2010-5, British Columbia Geological Survey, Geoscience Map 2010-1, and Geological Survey of Canada, Open File 6476, scale 1:500,000.

Loucks, R.R., 2014, Distinctive composition of copper-ore-forming arc magmas: Australian Journal of Earth Sciences, v. 61, p. 5–16.

Lougheed, H.D., McClenaghan, M.B., Layton-Matthews, D., and Leybourne, M.E., 2020, Exploration potential of fine-fraction heavy mineral concentrates from till using automated mineralogy: A case study from the Izok Lake Cu-Zn-Pb-Ag VMS deposit, Nunavut, Canada: Minerals, v. 10, article 310.

Lowell, J.D., and Guilbert, J.M., 1970, Lateral and vertical alteration-mineralization zoning in porphyry ore deposits: Economic Geology, v. 65, p. 373–408.

Mao, M., Rukhlov, A.S., Rowins, S.M., Spence, J., and Coogan, L.A., 2016, Apatite trace element compositions: A robust new tool for mineral exploration: Economic Geology, v. 111, p. 1187–1222.

Mao, M., Rukhlov, A.S., Rowins, S.M., Hickin, A.S., Ferbey, T., Bustard, A.L., Spence, J., and Coogan, L.A., 2017, A novel approach using detrital apatite and till geochemistry to identify covered mineralization in the TREK area of the Nechako Plateau, British Columbia: Geological Association of Canada Special Papers, v. 50, Mineralogical Association of Canada Topics in Mineral Sciences, v. 47, p. 191–243.

Massey, N.W.D., MacIntyre, D.G., Desjardins, P.J., and Cooney, R.T., 2005, Geology of British Columbia: British Columbia Ministry of Energy, Mines and Petroleum Resources, British Columbia Geological Survey, Geoscience Map 2005-3, scale 1:1,000,000.

McDonough, W.F., and Sun, S., 1995, The composition of the Earth: Chemical Geology, v. 120, p. 223–253.

McMillan, W.J., Anderson, R.G., Chan, R., and Chow, W., 2009, Geology and mineral occurrences (minfile), Guichon Creek batholith and Highland Valley porphyry copper district, British Columbia: Geological Survey of Canada, Open File 6079, scale 1:100,000 and 1:150,000.

Meyer., C., and Hemley, J.J., 1967, Wall rock alteration, *in* Barnes, H.L., ed., Geochemistry of hydrothermal ore deposits, 1st ed.: Holt Rinehart and Winston, New York, p. 166–235.

Migdisov, A.A., Williams-Jones, A.E., and Wagner, T., 2009, An experimental study of the solubility and speciation of the rare earth elements (III) in fluoride- and chloride-bearing aqueous solutions at temperatures up to 300°C: Geochimica et Cosmochimica Acta, v. 73, p. 7087–7109.

Mihalasky, M.J., Bookstrom, A.A., Frost, T.P., and Ludington, S., with contributions from Logan, J.M., Panteleyev, A., and Abbott, G., 2011, Porphyry copper assessment of British Columbia and Yukon Territory, Canada: United States Geological Survey, Scientific Investigations Report 2010-5090-C, 128 p.

Mills, S.J., Hatert, F., Nickel, E.H., and Ferraris, G., 2009, The standardisation of mineral group hierarchies: Application to recent nomenclature proposals: European Journal of Mineralogy, v. 21, p. 1073–1080.

Natural Resources Canada, 2021, Canada's critical minerals list 2021: https://www.nrcan.gc.ca/sites/nrcan/files/mineralsmetals/pdf/Critical_Minerals_List_2021-EN.pdf.

Norman, D.K., Parry, W.T., and Bowman, J.R., 1991, Petrology and geochemistry of propylitic alteration at southwest Tintic, Utah: Economic Geology, v. 86, p. 13–28.

Orovan, E., and Hollings, P., 2020, Exploring the green rock environment: An introduction: Economic Geology, v. 115, p. 695–700.

Panteleyev, A., Bailey, D.G., Bloodgood, M.A., and Hancock, K.D., 1996, Geology and mineral deposits of the Quesnel River-Horsefly map area, central Quesnel trough, British Columbia: British Columbia Ministry of Employment and Investment, Bulletin 97, 156 p.

Paradis, S., Jackson, S.E., Petts, D., Simandl, G.J., and D'Souza, R.J., 2020, Distribution of trace elements in pyrite of carbonate-hosted sulphide deposits of southern British Columbia, Canada: Geological Survey of Canada, Bulletin 617, p. 129–163.

Pisiak, L.K., Canil, D., Lacourse, T., Plouffe, A., and Ferbey, T., 2017, Magnetite as an indicator mineral in the exploration of porphyry deposits: A case study in till near the Mount Polley Cu-Au deposit, British Columbia, Canada: Economic Geology, v. 112, p. 919–940.

Plouffe, A., and Ferbey, T., 2016, Till geochemistry, mineralogy and textural data near four Cu porphyry deposits in British Columbia: Geological Survey of Canada, Open File 8038, and British Columbia Geological Survey, Geofile 2016-10, 1 zip file.

——2017, Porphyry Cu indicator minerals in till: A method to discover buried mineralization: Mineral Association of Canada Topics in Mineral Sciences, v. 47, Geological Association of Canada Special Papers, v. 50, p. 129–159.

——2018, Surficial geology of the Highland Valley Copper mine area (parts of 92-I/6, 7, 10 and 11), British Columbia: British Columbia Ministry of Energy, Mines and Petroleum Resources, British Columbia Geological Survey, Geoscience Map 2018-01, scale 1:50,000.

Plouffe, A., Ferbey, T., Hashmi, S., and Ward, B.C., 2016, Till geochemistry and mineralogy: Vectoring towards Cu porphyry deposits in British Columbia, Canada: Geochemistry: Exploration, Environment, Analysis, v. 16, p. 213–232.

Plouffe, A., Acosta-Góngora, P., Kjarsgaard, I.M., Petts, D., Ferbey, T., and Venance, K.E., 2021a, Detrital epidote chemistry: Detecting the alteration footprint of porphyry copper mineralization in the Quesnel terrane of the

Canadian Cordillera, British Columbia: Geological Survey of Canada, Bulletin 616, p. 137–157.
Plouffe, A., Wilton, D.H.C., McNeil, R., and Ferbey, T., 2021b, Automated indicator-mineral analysis of the fine-sand, heavy-mineral concentrate fraction of till: A promising exploration tool for porphyry copper mineralization: Geological Survey of Canada, Bulletin 616, p. 203–223.
Plouffe, A., Kjarsgaard, I.M., Ferbey, T., Wilton, D.H.C., Petts, D.C., Percival, J.B., Kobylinski, C.H., and McNeil, R., 2022, Detecting buried porphyry Cu mineralization in a glaciated landscape: A case study from the Gibraltar Cu-Mo deposit, British Columbia, Canada: Economic Geology, v. 117, p. 777–799.
Plouffe, A., Petts, D.C., Kjarsgaard, I.M., and Polivchuk, M., 2023, Laser ablation inductively coupled plasma mass spectrometry mapping of porphyry-related epidote from south-central British Columbia: Geological Survey of Canada, Open File 8968, 1 .zip file.
Rees, C., Gillstrom, G., and Riedell, K.B., 2020, The Mount Polley porphyry copper deposit, south-central British Columbia: Canadian Institute of Mining, Metallurgy and Petroleum, Special Volume 57, p. 567–600.
Richards, J.P., 2011, Magmatic to hydrothermal metal fluxes in convergent and collided margins: Ore Geology Reviews, v. 40, p. 1–26.
Rukhlov, A.S., Plouffe, A., Ferbey, T., Mao, M., and Spence, J., 2016, Application of trace-element compositions of detrital apatite to explore for porphyry deposits in central British Columbia: British Columbia Ministry of Energy and Mines, British Columbia Geological Survey, Geological Fieldwork 2015, Paper 2016-1, p. 145–179.
Schiarizza, P., 2015, Geological setting of the Granite Mountain batholith, south-central British Columbia: British Columbia Ministry of Energy and Mines, British Columbia Geological Survey, Geological Fieldwork 2014, Paper 2015-1, p. 19–39.
Schroeter, T.G., ed., 1995, Porphyry deposits of the northwestern Cordillera of North America: Montréal, Canadian Institute of Mining, Metallurgy and Petroleum, 888 p.
Seedorff, E., Barton, M.D., Stavast, W.J.A., and Maher, D.J., 2008, Root zones of porphyry systems: Extending the porphyry model to depth: Economic Geology, v. 103, p. 939–956.
Sharman, L., Lang, J., and Chapman, J., eds., 2020, Porphyry deposits of the northwestern Cordillera of North America: A 25-year update: Canadian Institue of Mining, Metallurgy and Petroleum, Special Volume 57, 726 p.
Sherlock, R., and Trueman, A., 2013, NI 43-101 technical report for 2012 activities on the Woodjam South property: Cariboo Mining Division, British Columbia, Gold Fields Horsefly Exploration Group and Consolidated Woodjam Copper Corporation, 158 p.
Sherlock, R., Blackwell, J., and Skinner, T., 2013, NI 43-101 technical report for 2012 activities on the Woodjam North property: Cariboo Mining Division, British Columbia, Gold Fields Horsefly Exploration Group, Consolidated Woodjam Copper Corporation, 275 p.
Shewchuk, C., Ferbey, T., and Lian, O.B., 2020, Detecting porphyry Cu-Mo mineralization using major oxides and pathfinder elements in subglacial till, Highland Valley mine area, south-central British Columbia: British Columbia Ministry of Energy, Mines and Petroleum Resources, British Columbia Geological Survey, Geological Fieldwork 2019, Paper 2020-01, p. 169–187.
Sillitoe, R.H., 2010, Porphyry copper systems: Economic Geology, v. 105, p. 3–41.
Sinclair, W.D., 2007, Porphyry deposits: Geological Association of Canada, Mineral Deposit Division, Special Publication 5, p. 223–243.
Spiegel, C., Siebel, W., Frisch, W., and Berner, Z., 2002, Nd and Sr isotopic ratios and trace element geochemistry of epidote from the Swiss Molasse basin as provenance indicators: Implications for the reconstruction of the exhumation history of the Central Alps: Chemical Geology, v. 189, p. 231–250.
Sutherland Brown, A.E., ed., 1976, Porphyry deposits of the Canadian Cordillera: Montréal, Canadian Institute of Mining and Metallurgy, 510 p.
Teck, 2022, Annual information form: https://www.teck.com/media/2022-AIF.pdf.
van Straaten, B.I., Mostaghimi, N., Kennedy, L.A., Gallagher, C., Schiarizza, P., and Smith, S., 2020, The deformed Gibraltar porphyry copper-molybdenum deposit, south-central British Columbia, Canada: Canadian Institute of Mining, Metallurgy and Petroleum, Special Volume 57, p. 546–566.
Wilkinson, J.J., Cooke, D.R., Baker, M.J., Chang, Z., Wilkinson, C.C., Chen, H., Fox, N., Hollings, P., White, N.C., Gemmell, J.B., et al., 2017, Porphyry indicator minerals and their mineral chemistry as vectoring and fertility tools: Geological Survey of Canada, Open File 8345, p. 67–77.
Wilkinson, J.J., Baker, M.J., Cooke, D.R., and Wilkinson, C.C., 2020, Exploration targeting in porphyry Cu systems using propylitic mineral chemistry: A case study of the El Teniente deposit, Chile: Economic Geology, v. 115, p. 771–791.

Alain Plouffe is a retired Quaternary geologist from the Geological Survey of Canada (GSC). He has over 30 years of experience combining glacial geology applied to mineral exploration in the Canadian Cordillera. He holds an M.Sc. degree from Carleton University and a Ph.D. degree from the University of Montreal. He led surficial geology mapping projects and regional till geochemical and mineralogical surveys in British Columbia, Yukon, and northwest Alberta, with direct applications for the discovery of buried mineralization. He is currently pursuing research on developing mineral exploration methods for porphyry mineralization in glaciated landscape studying examples from the Canadian Cordillera.